DOI 10.1007/s11106-024-00403-x
Powder Metallurgy and Metal Ceramics, Vol. 62, Nos. 7-8, November, 2023 (Ukrainian Original Vol. 62, Nos. 7-8, July-August, 2023)

RESEARCH ADVANCES IN CLOSE-COUPLED ATOMIZER FLOW AND ATOMIZING MECHANISMS

Min Zhang,[1,3] Zhaoming Zhang,[2] and Qiusheng Liu[1]

UDC 532.525:621.762.2

As component manufacturing technology evolves, more demands are placed on improved performance of metal/alloy powders in medical, military, machining, and 3D printing applications. High-quality powders are characterized by low oxygen content, precise alloy composition, small particle size, and high particle sphericity. Coupled gas atomization powder preparation technology is an ideal choice for preparing high-quality powders with high atomization efficiency, low oxygen content, and high cooling rate. However, this powder preparation technology's multiphase flow and multiscale coupling is a complicated physical process. In addition, the mechanism of atomization has not yet been fully understood. Thus, there is no consensus on the atomization phenomena and atomization mechanisms. Close-coupled gas atomization powder preparation technology is facing great challenges in the field of low-cost mass production of high-quality powders. Therefore, it is expected to improve the close-coupled gas atomized powder preparation technology and achieve breakthroughs in atomization principle, such as high-efficiency gas atomization technology, intelligent control of the high-efficiency gas atomization process, and so on. In this respect, this review summarizes the atomizer structures, gas atomization flow field-testing technologies, and gas atomization flow field numerical simulations based on relevant literature. In addition, the gas atomization mechanism of the closely coupled atomizers will be analyzed. Finally, several research directions are proposed for further in-depth studies on the atomization characteristics and mechanisms of close-coupled vortex loop slit atomizers.

Keywords: *gas atomization, close-coupled atomizer, atomization flow field, atomization mechanism, vortex loop slit atomizer.*

INTRODUCTION

The demand for materials has increased with industrial development. Firstly, materials need to be high-performing to meet the needs of the aerospace, automotive, healthcare, and electronics industries. On the other hand, the process used to produce the materials should be simple, economical, and energy-saving. Because of their advantages in producing powders with precise composition, small grains, and uniform structure, few or no cuttings, and high raw material utilization, various powder metallurgy-based materials and parts manufacturing technologies have been increasingly applied in various fields.

[1]Key Laboratory of Microgravity (National Microgravity Laboratory), Institute of Mechanics, Chinese Academy of Sciences, Beijing 100190, People's Republic of China. [2]College of Aerospace Engineering, Nanjing University of Aeronautics and Astronautics, Nanjing 210016, People's Republic of China.

[3]To whom correspondence should be addressed; e-mail: zhangmin@imech.ac.cn.

Published in Poroshkova Metallurgiya, Vol. 62, Nos. 7–8 (552), pp. 24–56, 2023. Original article submitted February 13, 2023.

Product performance is largely determined by the raw material used in powder metallurgy technology, namely the metal powder. That is, the efficiency of the production technology and the product quality can be directly influenced by the morphology, particle size and distribution, composition, and microstructure of the metal powder [1]. High-quality and cost-effective powders can not only expand the application areas of powders but also improve the production method in the powder metallurgy industry. The development of high-quality powder preparation methods has become one of the most active leading research topics at present. The characteristics of high-quality powders are small particle size, uniform composition, and spherical particles [2, 3]. Therefore, various methods used to prepare metallic powders have attracted considerable attention. As a result, many scientific research units and enterprises are dedicated to developing and improving metal powder preparation technologies.

Based on the preparation technique, the methods of metal powder preparation can be classified into the atomization method, reduction method, electrolysis method, carbonyl decomposition method, and grinding method [4]. The metal powders produced by atomizing, reducing, and electrolyzing methods are commonly used as raw materials in the powder metallurgy industry. Electrolysis and reduction methods are limited to producing pure metallic powders; they do not apply to alloying powders. In contrast to these methods, alloy powders can be produced by the atomization method, and the morphology of metal/alloy powders can be controlled by modern atomization processes. In addition, with the continuous development and optimization of atomizer structures, atomization efficiency has increased significantly. As a result, atomization is gradually becoming an important method for the preparation of metal/alloy powders.

Atomization involves mechanically breaking the molten metal into droplets less than approximately 150 μm in diameter. There are several types of atomizing processes. According to the method of breaking the metal melt, atomization methods can generally be divided into two-stream, centrifugal, ultrasonic, and electrode-induced atomization methods, in which the metal melt is broken by high-pressure water flow and airflow, a centrifugal force, ultrasound, and high-frequency current, respectively. Each of these atomization methods has its specific characteristics, and all of them have been in use in industrial production. Water (gas) atomization methods have become the most important industrial methods of metal powder preparation. They require simple production equipment and techniques, consume little energy, and facilitate large batch operations.

Among the atomization-based methods of powder preparation, the water atomization method is an economical method. It has high atomization efficiency, and the atomizing medium (water) is inexpensive and easy to use. Currently, the water atomization method is mainly applied to the production of steel powders, matrix powders for diamond tools, pre-alloy powders for oil bearings, powders for hard surfaces, and Fe- and Ni-based magnetic powders. However, because the specific heat capacity of water is much higher than that of gas, the crushed metal melt becomes irregular due to overcooling during water atomization, which affects the sphericity of metal powder. Upon contact with water, some high-activity metals and alloys react immediately. When the powder comes into contact with water during water atomization, the oxygen content of the metal/alloy powder increases. These challenges limit the production of high sphericity, low oxygen metal powders using water atomization methods.

One of the most important industrial methods of powder preparation is gas atomization. Essentially, the metal melt is broken into small droplets using a pressurized gas atomizer and cooled into metal powder particles. Because inert gases can be used as atomizing media, the melt can be protected by vacuum or inert gases, thereby reducing the contact between the metal melt and oxygen. This is conducive to a reduction in the oxygen content of the metal powder being produced. Furthermore, due to the relatively low specific heat capacity of the atomizing gas, it provides sufficient time for the metal melt drops to nodulate, increasing the sphericity of the metal powder and improving the technical performance of the prepared metal powder. Therefore, gas atomization is an ideal method for producing high sphericity, low oxygen-containing metal powders. However, there are some shortcomings of the gas atomization method. Since the energy of a high-pressure air flow is significantly lower than that of a high-pressure water flow, the gas atomization method has a lower atomization efficiency of the metal melt than that of the water atomization method. As a result, the cost of preparing the metal powder rises. Therefore, the focus of many scientific researchers is on the improvement of gas atomization efficiency.

Theoretically, high-quality powders can be produced with the close-coupled gas atomization powder preparation technology. It enables high atomization efficiency, low oxygen content of the powder, and high cooling rate. An atomizer is a core component of the gas atomization equipment, and its structure can significantly affect the jet flow field of the atomization media and the atomization efficiency. Therefore, for gas atomization of metal melts, the design optimization of the atomizer structure is crucial. That is, the close coupling gas atomization powder preparation technology has all the advantages when the structure parameters of the close coupling atomizer and the atomization technology parameters are optimized.

At present, the relevant research units and production enterprises maintain a high level of technology confidentiality, but they have not yet determined the specific atomizer structural parameters and atomization technological parameters of industrial significance based on the relevant studies and patents. Therefore, many scientific research institutions are focusing on improving the production efficiency of high-quality gas atomization powders based on the existing close-coupled atomizers to realize industrial production, and this research is thus of high practical significance.

Up to now, there have been three main types of studies on the atomization of gases. First, experimental studies: the powdering process based on gas atomization is physically and comprehensively studied using optical tests and computers. The second type includes numerical calculations on the flow field structure of the gas atomization and the atomization mechanisms by using computers. Theoretical analysis is the third type: the gas atomization powder preparation process is under investigation based on the existing theories.

Therefore, this paper comprehensively reviews and summarizes the experimental technologies, numerical calculations, and research progress related to gas atomization.

METAL POWDER PREPARATION TECHNIQUES BASED ON GAS ATOMIZATION AND THE DEVELOPMENT COURSE

Metal powder preparation based on gas atomization involves breaking a molten metal liquid into small molten droplets by a high-velocity jet from the atomizer. These small molten droplets are then cooled to metal powder particles in an airflow environment. As shown in Fig. 1, atomization is a process that converts the kinetic energy of the gases into the surface energy of the molten metal. The increase in the utilization of the kinetic energy of the gases is the key to the increase in atomization efficiency. The most direct factor affecting atomization efficiency is the atomizer structure. Therefore, many scientific research institutions and enterprises have been

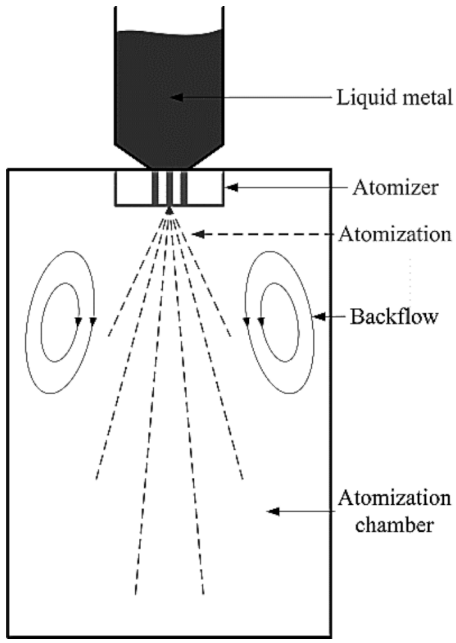

Fig. 1. Simplified schematic of the powder preparation process based on gas atomization

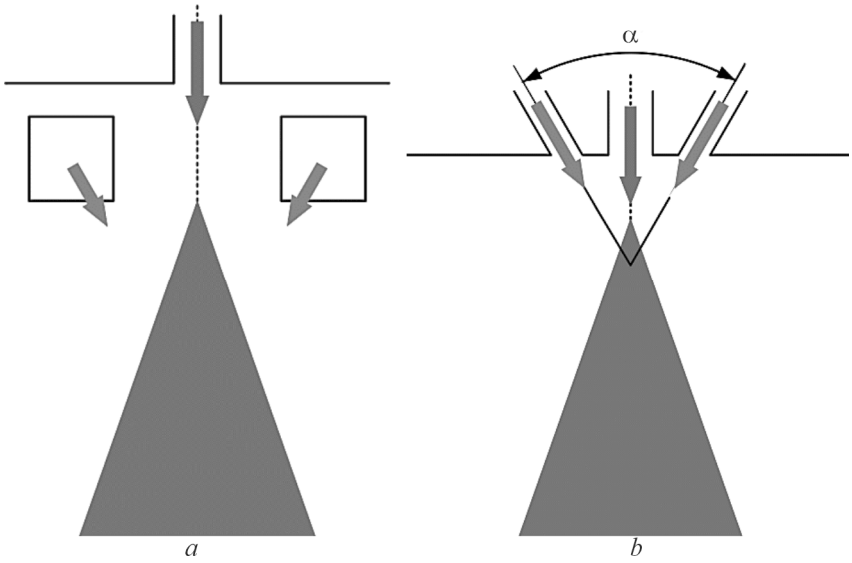

Fig. 2. Schematic of gas atomization of free-fall (*a*) and restricted (*b*) atomizers

engaged in the reform of gas atomization technology through the development and optimization of atomizer structures. The development status of atomizer and its structure is briefly introduced below.

Metal powders have been prepared by the gas atomization method since the early 1820s. In the 1830s, two types of atomizer structures were designed: Free-fall and restricted atomizers, as shown in Figs. 2*a* and *b*, respectively [5]. Both of these atomizers are still in use today, and each has its specific advantages and disadvantages. The free-fall atomizer has a simple design and manufacture, facilitates a stable atomization process, and does not easily clog the nozzle. However, it has a low atomization efficiency and is only applicable to the production of metal powders with a particle size of 50–300 μm [6]. The restricted atomizer is designed with a compact structure. The melt delivery tube (MDT) is closely connected to the atomizer so that the molten metal liquid is immediately atomized as it flows out of the center hole in front of the MDT. Thus, high atomization efficiency is achieved. However, the design and manufacturing of the MDT are complex. In the atomizing process, the restricted atomizer is less stable than the free-fall atomizer. Therefore, the development of gas atomization technology has been slow in the subsequent period. For example, when General Motors started mass production of oil pump gears based on powder metallurgy technology, it still prepared Fe powder by the reduction method.

During World War II, Mannesmann (Germany) proposed a more efficient method than the reduction method for producing Fe powders. The demand for Fe-based sintered parts was increasing rapidly. Mannesmann produced a high-performance Fe powder using a method in which Fe was crushed and melted using a conical flow of air. This method is the Mannesmann method, and its basic design and principles are now in use [7, 8]. The Mannesmann method was soon widely adopted in Europe because it is more efficient and easier to control than the reduction method in the preparation of Fe powders.

In 1954, Watinson improved the structure of the atomizer based on the Mannesmann method; the molten Fe liquid was atomized by means of compressed air through an annular slit atomizer. However, the metal powder could be easily oxidized by the atomization medium (air), which reduced the purity of the metal powder [7].

In 1967, Joyce carried out a gas atomization experiment on a super alloy melt and found that the alloy melt could be atomized in a stable manner after passing through a superheating threshold. In addition, as the inclusion angle of the atomizing air stream increases, the particle size of the alloy powder decreases [2].

In 1968, the design of a subsonic and supersonic gas jet atomizing nozzle was further studied and optimized by Nichiporenko and Naida [9].

In 1971, Klar and Shafer [7] did a comparative analysis of the advantages and disadvantages of various gas atomizers-external hybrid, restricted, and free-fall. They found that the restricted atomizer was more efficient than the free-fall atomizer, but it tended to clog the MDT with molten metal.

In 1975, Naida compared three types of atomizers that are widely used in practice, namely restricted, free-falling, and flat cone. He found that the free-fall atomizer was the most suitable because the pressure at its outlet is the lowest. This is most beneficial for the inhalation of the metal melt into the high-speed airflow [3].

From the end of the 1970s to the beginning of the 1980s, computers and modern control technologies were applied for developing gas atomization technologies for powder preparation. Moreover, with the continuous increase in the number of studies on gas atomization mechanisms, many new gas atomization technologies have been developed, which are entering the boom stage. During this period, gas atomization-based metal powder preparation methods were developed as the primary method. The metal powders produced accounted for 30-50% of the total metal powder yield worldwide [10].

In 1980, Professor Grant from MIT (USA) optimized the ultrasonic atomization device which was invented in Sweden, and produced metal powders with small particles and rapid cooling and solidification effects (the average particle size is less than 50 μm) [11].

In 1981, Rutharde [12] manufactured a laminar flow atomization device that could prepare metal powders with smaller particles at a lower cost. Several years later, Walz [13] gradually optimized it and developed laminar flow atomization.

In 1985, Anderson of the Ames Laboratory in Iowa, USA, developed the high-pressure gas atomization (HPGA) technology, which is based on a restricted ring hole atomizer. With this technology, an ultrasonic velocity air flow is achieved by using a high-pressure gas (17.3 MPa), which breaks up the metal melt [14]. In this paper, the suction pressure intensity (ΔP) at the front end of the MDT was shown to be related to the atomization gas pressure. In addition, the particle size of the prepared metal powder decreases with a decrease in ΔP. The average particle size is less than 20 μm. This indicates that the energy exchange between atomizing gas and metal melt increases accordingly.

In 1986, Miller [15] studied a restricted atomizer. This increased the efficiency of converting the kinetic energy of the gases to the surface energy of the metal melt. Based on this concept, he designed a close-coupled atomizer that could minimize the distance from the atomizing gas jet outlet to the molten metal. Because the metal powder produced by the close-coupled atomizer has small particles (the average particle size is less than 30 μm), a narrow particle size distribution range, and a high cooling speed (10^3–10^7 K/s), it is conducive to rapid condensation and production of amorphous powders. Currently, close coupled atomization has become the conventional gas atomization technology for powder preparation, widely studied and applied in industry.

In 1988, Ünal et al. of Imperial College London, United Kingdom [16] developed an atomization technology for gas atomization as shown in Fig. 3. In this technology, a Laval atomizer is used to generate an ultrasonic velocity air stream to break up the molten metal. The molten metal is then sprayed from the top of the atomizer. The average particle size (less than 25 μm) of the metal powder produced by this atomizing technology is proportional to the mass flow rate of the metal melt. Increasing the atomizing gas pressure does not significantly

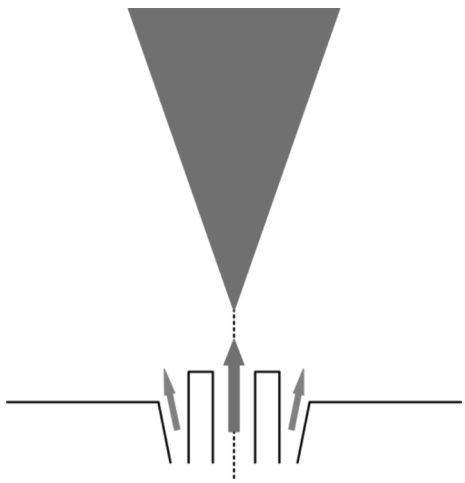

Fig. 3. Schematic atomization model of a gas up-jet atomizer

affect the average particle size of the metal powder when the mass flow rates of the atomizing gas and the metal melt are fixed.

In 1990, Hopkins of PSI Company (UK) optimized the structure of a close-coupled loop slit atomizer to generate ultrasonic velocity at the atomization gas outlet. That is, ultrasonic close-coupled atomization technology can be realized by obtaining high-velocity atomizing gases at low atomizing gas pressure [17]. A characteristic of this atomization technology is that the mass flow rate of the metal melt can be more than 0.5 L/min. This is advantageous for low-cost industrial production. The prepared metal powder has a high cooling rate (10^3–10^7 K/s). Therefore, this method is useful for preparing metal powders with a high condensation rate or amorphous structures.

In 1993, Gerking of Nonoval (Germany) significantly improved the close-coupled atomizer based on Walz et al.'s studies, proposing the laminar ultrasonic atomization concept [18]. A feature of this atomization technology is that the atomized air stream hits the metal melt at no other angle than parallel (0°) to the metal melt. Due to the synergy between the shear force and the squeezing effect of the atomized airflow, the metal melt deforms during atomization. This means that the diameter of the metal melt is continuously reduced, followed by a laminar fibrillation process. When the molten metal leaves the atomizer, the external pressure immediately decreases and the internal-external pressure difference increases. This causes the molten metal to break by self-excitation. The average particle size of metal powder produced by laminar ultrasound atomizing technology is less than 10 μm. In 2021, Xu et al. [19] systematically investigated the atomization gas flow, primary and secondary fracture mechanisms, and particle morphology related to the laminar gas atomization process by numerical simulation and experimental analysis.

In 1997, Strauss [20] proposed the concept of thermal gas atomization based on close-coupled gas atomization technology according to the ideal gas state equation: $PV = nRT$. For a given constant pressure intensity of the atomizing gas, increasing its temperature can facilitate the swelling of the atomizing gas entering the atomizing chamber, thereby increasing its velocity. The average particle size is less than 20 μm for metal powders produced by thermal gas atomization technology. In 2020, Hussain et al. [21] for the first time applied the thermal gas atomization technology to the spray-forming process to improve the quality of the spray-formed tubular deposits. In 2021, Wang et al. [22] studied the influence mechanism of gas temperatures (300, 400, 500, and 600 K) on gas atomization by simulating the integral atomization process of the close-coupled nozzle in vacuum induction gas atomization.

In 2002, Schulz of Widerflow Metal Powder Manufacturing Company (Germany) combined water atomization and gas atomization to overcome their shortcomings. As a result, a new atomization-based powder preparation technology with low atomizing gas consumption and excellent performance was developed [23]. The traditional water atomization technology usually requires atomization pressure higher than 50 MPa, and the oxygen content in the prepared metal powder is high. The gas atomization technology consumes a large amount of atomizing gas, and

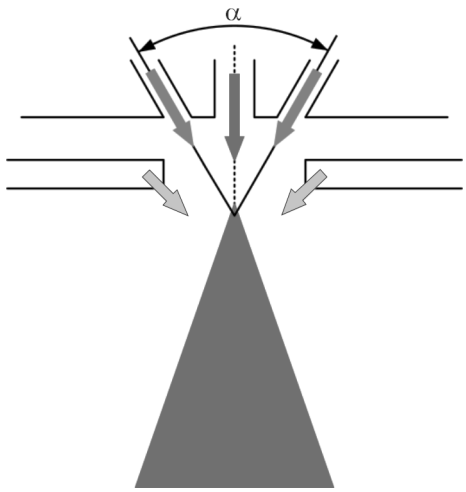

Fig. 4. Schematic of the atomization method of a low-pressure gas and water atomizer

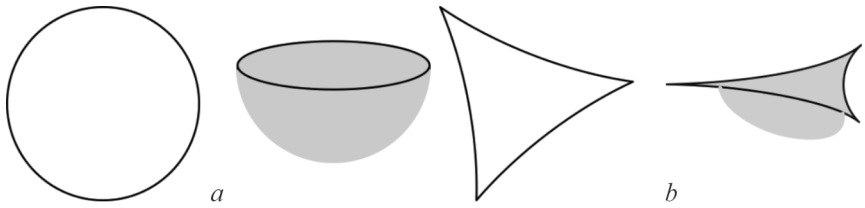

Fig. 5. Three-dimensional simulation diagram of (*a*) annular and (*b*) curvilinear triangular nozzles for gas atomization

the particle size distribution range of the prepared metal powder is wide. As shown in Fig. 4, during atomization, the metal melt is first pre-atomized with a low-pressure atomizing gas. After obtaining the liquid metal film in the laminar state, water atomization is performed. The metal powder produced by this method has smaller particles (the average particle size is less than 20 μm) and lower oxygen content compared to the metal powder produced by water atomization or gas atomization. Furthermore, the gas consumption is lower.

In 2005, McGuinness et al. [24] performed a three-dimensional (3D) simulation of the atomizing nozzle using numerical simulations and discussed the methods to decrease the droplet diameter under a given pressure difference. By studying the relationship between the pressure difference at the end of the nozzle and the volume and final diameter of the droplets, they found that the surface tension limits the decrease in the diameter of the atomized droplets. In particular, the pressure difference at the nozzle end is related to the shape of the nozzle during droplet formation.

The traditional nozzle is a round or annular tube, as shown in Fig. 5*a*. Due to the difference in the radius of curvature, the droplets obtained from the non-annular nozzle have a significantly smaller diameter than those obtained from the annular nozzle at the same pressure difference. This difference is more significant when a triangular nozzle is used, as shown in Fig. 5*b*. The droplet diameter is 33% smaller than that obtained with the annular nozzle under the same conditions, that is, the critical pressure difference. Therefore, this result promotes the gradual optimization of the structural design of the atomizing nozzle and provides a new idea for the study of gas atomization technology.

In 2008, Czisch and Fritsching (Germany) [25] performed a numerical simulation and calculation of the flow field in a twin-fluid composite atomizer and optimized the double-layer composite gas atomization, as shown in Fig. 6. This atomization technology involves a close-coupled and free-fall atomizers. The close-coupled atomizer was located at the top and connected to the crucible and MDT referred to as the primary atomizer. The free-fall atomizer was located below the close-coupled atomizer, referred to as the secondary atomizer. During the atomization, the

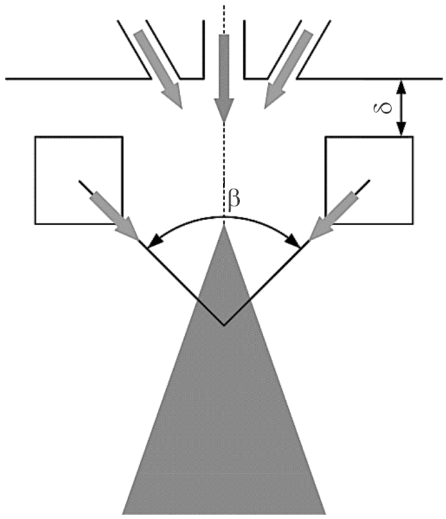

Fig. 6. Schematic of gas atomization in a twin-fluid composite atomizer

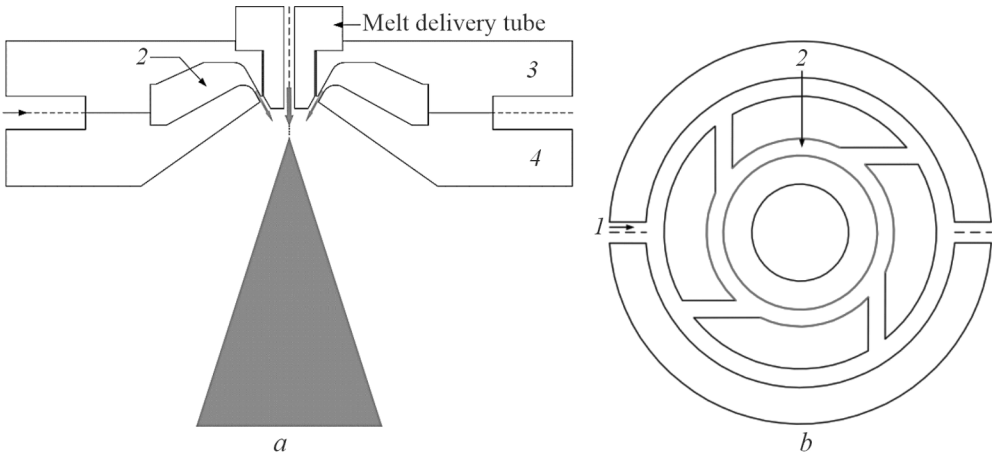

Fig. 7. Schematic of gas atomization of a close-coupled vortex loop slit (*a*) longitudinal section and (*b*) cross section

close-coupled atomizer ensures a stable outflow of the metal melt and its inflow to the gas flow field in the free-fall atomizer. The primary and secondary atomizers facilitate the flow diversion in primary and secondary atomization, respectively. The mass flow rate of the atomizing gas was controlled by adjusting its pressure in the gas inlet channels of both atomizers. The average particle size of metal powder prepared by the double-layer composite gas atomization technology is less than 33 μm.

In 2021, Prashanth et al. [26] studied the role of MDT position in atomization, i.e., its effect on the yield, mass median diameter, and spread of the particle size distribution. In 2022, Choi et al. [27] experimentally investigated the atomization of a water column by a gas jet flow (Reynolds number ~$O(10^4–10^5)$) issued from a two-stage annular nozzle. It was found that the key parameter to drive the atomization is the acceleration of the gas flow (velocity gradient) experienced by the falling water.

In 2021, Zhang [28] studied the gas flow field and atomization mechanism of a close-coupled vortex loop slit atomizer using experiments and numerical simulations, followed by optimization of the close-coupled vortex loop slit gas atomization, as shown in Fig. 7. The close-coupled vortex loop slit atomizer is a characteristic of this atomization technology, which can cause vortex motion of the atomizing media. The atomizer comprises a symmetric vertical gas inlet channel *1*, round cavity *2*, upper central cone *3*, and lower central cone *4*. The upper and lower central cones form an annular slit gas outlet, and the metal/alloy melt is input to the center hole of upper central cone *3* through the MDT. During atomization, the atomizing media is swirled in the circular cavity *2* and then sprayed from the annular slit gas outlet formed by the upper and lower central cones *3* and *4*, respectively. Then, the high-pressure gas atomizing media enters the atomizer through the gas inlet. When the metal/alloy melt flows out of the central hole at the front end of the MDT with some superheating, it is immediately atomized into microdroplets by the high-speed atomizing media sprayed from the atomizer's annular slit gas outlet. Finally, the micro-droplets are frozen into solid particles of powder during the flight.

Additive manufacturing (AM), referred to as 3D printing, has emerged popular in recent decades. The AM process implies layer-by-layer deposition of materials and fabricating products directly from a 3D model [29, 30]. Products with complex designs can be rapidly manufactured with high precision using this technology. Therefore, AM is widely used in industry and biomedicine [31, 32]. Due to the tremendous market growth of 3D printed parts and components, the demand for metal powders for AM printers has increased. This has led to quality issues and optimization of the atomization process. Powdered metals are the key ingredients in metallic AM and therefore in 3D printing [33, 34]. Gas atomization is currently the leading technology for producing metal powders for AM [35, 36]. Hence, it is of practical significance to increase the production efficiency of high-quality gas atomization powders based on existing atomization technologies.

EXPERIMENTAL STUDIES ON GAS ATOMIZATION FLOW FIELD IN THE ATOMIZER

Without the characterization of the atomization process using appropriate testing technologies, the atomization characteristics and mechanisms of an atomizer cannot be studied. Developing atomization characteristic two-phase flow testing technologies has gradually deepened the understanding of the gas atomization process. Atomization efficiency mainly depends on metal/alloy powder particle size and distribution, metal droplet velocity, temperature, and gas/liquid mass flow ratio. In-depth studies of atomization mechanisms must focus on many parameters, such as metal melt breakup mode, metal liquid film thickness, and disturbances caused by atomizing gas on the metal liquid film surface [37].

Early measurement methods of the flow field of the atomizer mainly include shadowing, Schlieren photography, sedimentation, freezing, and contact [38]. However, these methods do not allow for analyzing the atomization mechanisms in detail. Hence, advanced measurement methods and technologies are required to investigate the gas atomization process more comprehensively and thoroughly. In recent years, gas atomization detection techniques have been greatly influenced by the rapid development of computers and optical technologies. Optical inspection technology has been adopted in many studies on atomization characteristics and mechanisms of atomizers because it is convenient and accurate, and can facilitate dynamic testing without disturbing the flow field.

Currently, the major optical test methods used to study the atomization characteristics and mechanisms include laser Doppler velocimetry (LDV), phase Doppler particle analysis (PDPA), laser scattering method (LSM), laser-induced fluorescence (LIF), particle image velocimetry (PIV), and laser holography (LH). The following text briefly introduces the test principles, application conditions, and advantages and disadvantages of these methods.

In LDV, the velocity information of the microparticles in the flow field is determined from the Doppler shift in the scattered light of the moving microparticles in the flow field. That is, the difference between the frequency of light scattered from the particles moving in the flow field and the frequency of light incident on the particles is proportional to the particle velocity [39]. As a result, these two frequencies are accepted by the detector and are processed to obtain the time information of the particles moving in the flow field. Next, the distance between the interferometric fringes is used to obtain the distance information of the particles moving in the flow field. Since velocity is equal to distance/time or distance × frequencies, it is possible to obtain velocity information of the particles moving in the flow field.

LDV offers the following advantages: it has relatively high time resolution and the laser does not interfere with the flow field while measuring. It measures the velocity rather than the function of the velocity. In addition, it can be applied to conditions that are difficult to access or for which conventional instruments are not suitable. However, LDV has some drawbacks. It cannot provide instantaneous velocity information of the entire flow field because it measures the velocity distribution of the flow field from one spatial point to another. Also, LDV cannot measure low-velocity fields because the frequency shifts are small.

The PDPA method was proposed by Durst and Zare [40] in 1975. It is a further development of the LDV method. In particular, another photoelectric detector was added to the optical system of the LDV to facilitate simultaneous measurement of the velocity and diameter of the droplets in the flow field.

In PDPA of flow fields, droplet diameter measurement errors are caused by many aspects. These include the Gaussian distribution of energies in the beam [41], the presence of a wide range of droplets with a phase difference greater than 360°, droplet shape, overlapping signals from multiple droplets during volume testing, and multiple scattering and absorption of light among droplets [42]. Therefore, PDPA can only provide information about the local flow field, and cannot measure droplet diameters in flow field zones with high droplet concentrations. Acquiring information about the entire flow field takes considerable time.

Mie and Rayleigh scattering methods are the two types of LSM. In the Mie scattering method, a spherical droplet model is built following the Mie scattering theory, and the Fraunhofer diffraction principle is applied. Because the droplet shape and distribution laws significantly influence this model in the testing flow-field zone, the measurement results are restricted by the average diameter of the droplets in that zone. The Malvern laser particle analyzer is an extensively used atomization tester. As laser scatters on microparticle surfaces when passing through

the testing flow field, the average diameter of the droplets in that region can be obtained by measuring the energy distribution and intensity of scattered light. The acquired information is then transmitted to a computer terminal for processing. Rayleigh scattering operates via spray evaporation, and the temperature distribution is determined from the optical characteristics of the droplets. The density and temperature distribution in the testing flow field can be measured simultaneously. Due to the limitations of the intensity of the scattered light, Rayleigh scattering is only applicable to environmental conditions where there are significant differences in the droplet density in the atomization flow field [43].

In the LIF method, the temperature distribution of the droplets in the atomization flow field is determined by adding a fluorescent agent to the fluid or from the fluorescence characteristics of the fluid. Since the droplets in an atomizing flow field fluoresce when excited by a laser, the fluorescence information of the droplets is collected and analyzed to determine the temperature distribution of the droplets. In practical applications, however, LIF technology has some limitations. The calibration accuracy significantly affects the measurement results, and the LIF system is susceptible to changes in ambient temperature during the measurement.

Particle image velocimetry is a new, instantaneous, full-flow-field, flaky-light-based velocity testing method that was developed in the 1980s based on research achievements in computing, optical, and image analysis technologies [44]. The velocity-vector measurement principle in PIV is as follows. First, small tracer particles are uniformly dispersed in the fluid media. The tracer particles' size, material, and specific weight must be chosen appropriately to ensure their optimum flow with the fluid media. Subsequently, the laser beam is transformed into flaky light through a cylindrical optical lens. The testing flow-field region is lit twice continuously within a short pulse time interval. In addition, two successive images of the tracer particles on laser-irradiated flaky light planes are quickly recorded using high-resolution, cross-frame cameras. These two images are sent to an image acquisition card through a universal serial bus cable. Finally, the processor determines the displacement of each point or region within a pulse time interval using a cross-correlation algorithm and then calculates the velocity vector of the small tracer particles in the testing flow-field region. Currently, two-dimensional (2D) PIV technology is relatively well-developed. It has been extensively used to measure the flow fields of various complicated airflow structures, including rotating flows and disturbance flows. The 3D PIV technology has been commercially available [45]. The operating principle involves the acquisition of multiperspective time-series images of tracer particles in the flow field of the same testing region, following which a 3D spatial flow field is reconstructed after extracting the 2D flowing information from multiple perspectives.

The PIV technology is not only equipped with the precision and resolution of the single-point measurement method but also acquires the overall structure and instantaneous particle images of the plane flow field. Moreover, it can simultaneously measure the velocity, average velocity, pulsation velocity, and strain rate of the tracer particles in the entire testing flow-field region. Therefore, it overcomes the limitations of the spatial single-point measurement method and can instantaneously record the overall flow information of a plane. A comparative analysis of the velocity and vorticity fields of the tracer particles at several successive time instants would reveal the instantaneous process of unsteady flow and the flow details. In addition, the PIV technology offers the advantages of high spatial resolution, absence of disturbance to the testing flow field, and continuous measurement.

Zhang et al. [28, 46] and Kirar et al. [47] studied the atomizing gas flow field in a close-coupled vortex loop slit atomizer by PIV and obtained the velocity vector field on a central longitudinal section in an instantaneous gas flow field of the atomizer, as shown in Fig. 8.

The principle of LH is as follows. First, the light amplitude and phase information of the droplets in an atomization flow field is collected based on reference light beams. The intensity and phase differences when the two object light beams overlap with the reference light beam are evaluated to obtain the amplitude and phase distribution of the object light beams. Next, the light is diffracted through the hologram by holographic imaging to generate images of the objects. Finally, 3D images of the droplets in the testing flow-field region are obtained. Unlike traditional optical imaging technology, holographic imaging technology enables the acquisition of 3D images. In the optical imaging technology, only the light intensity distribution is recorded. Although LH has afforded many benefits after development and optimization over the years, it has some limitations.

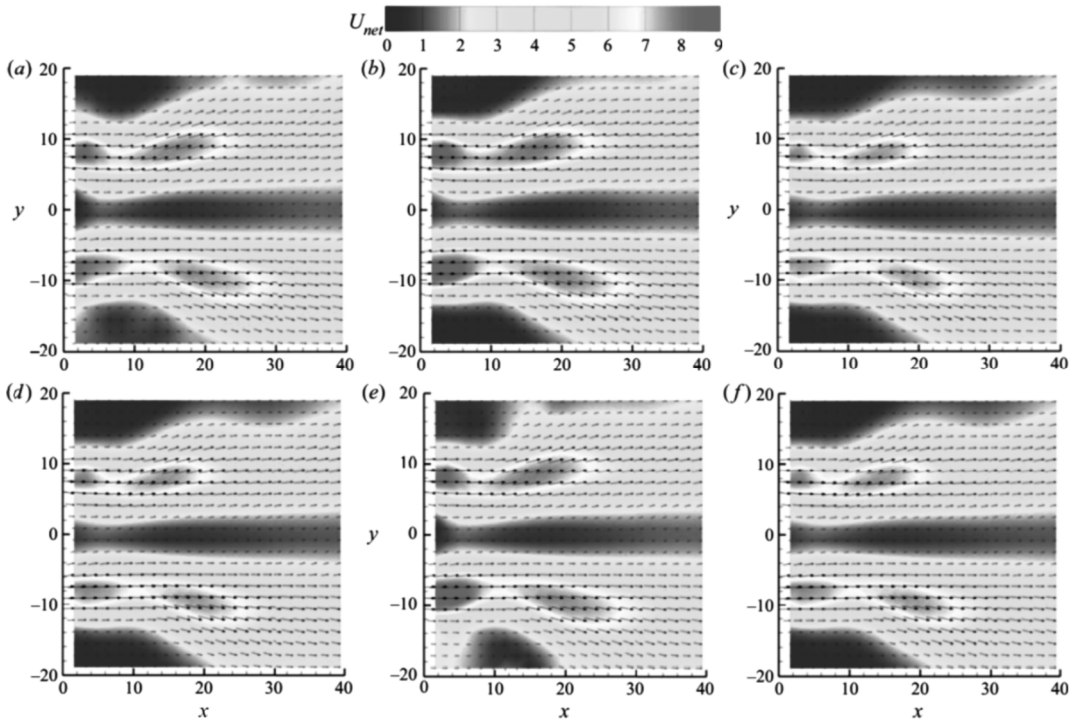

Fig. 8. Contours of the resultant velocity $U_{net} = \sqrt{U_x^2 + U_y^2}$ superimposed with velocity vectors at the $\overline{z}_d = 0$ plane for $We = 11.40$ and $Sw = 0.82$: the x and y labels are in mm, and U_{net} is in m · s^{-1} [47]

The aforementioned optical testing methods are noncontact measurement techniques, which do not cause any disturbance to the testing flow field. The progress in noncontact measurement technologies is attributed to the rapid development of modern computers. That is, atomization-flow-field-based two-phase flow testing technologies are based on the integrated application of computer automation and smart technologies, such as high-speed data acquisition, parallel processing, and real-time control. Therefore, the rapid development of modern computers has become crucial for studying the atomizing characteristics and mechanisms of atomizers. Experimental studies of gas atomization processes based on optical testing technologies have attracted considerable research attention with the rapid development of optical technologies. As a result, optical testing technologies will continue to be used to investigate sprayer characteristics and mechanisms.

GAS-ATOMIZATION MECHANISM STUDIES OF CLOSE-COUPLED ATOMIZERS

In the gas-atomization-based powder preparation process, a large-volume, continuous-phase liquid is converted into small-volume, discrete-phase droplets. The discretization is caused by the external kinetic energy. That is, the high-velocity gas breaks the continuous-phase liquid column into small droplets and liquid segments, thereby substantially increasing the surface area of the liquid column. Moreover, a large quantity of heat in the liquid column is quickly transmitted by the high-velocity atomizing gas, thereby rapidly cooling the liquid column. The gas atomization of the liquid takes place rapidly, and the atomizing gas jet's velocity is high, accompanied by a drastic exchange of momentum and energy between the gas and liquid phases. The entire gas atomization-based powder preparation process is a complex, unsteady interaction process between multiphase flows under an extremely turbulent state. This makes the modeling analysis difficult [48]. Currently, the whole gas atomization-based powder preparation process can be divided into two stages: primary and secondary [49]. The research progress in the two stages is briefly analyzed and summarized. As shown in Fig. 9, we have also summarized the major achievements and breakthroughs.

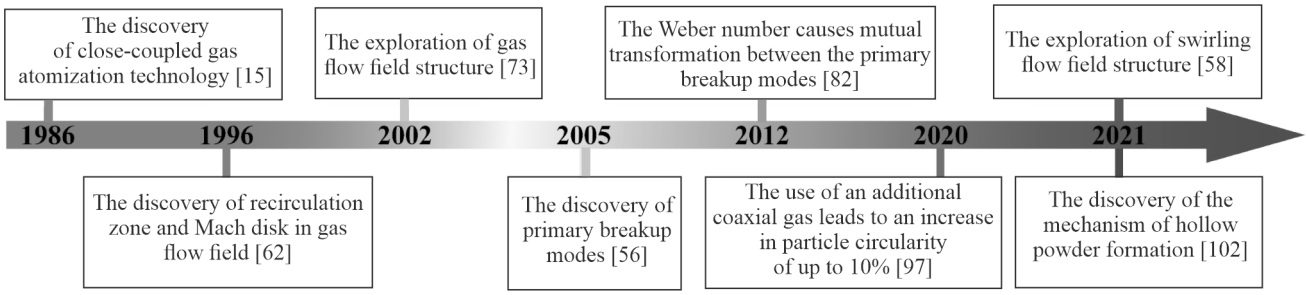

Fig. 9. Milestone in close-coupled gas atomization mechanisms

Deformation of the Liquid Column and Primary Break-up. The metal melt flowing out of the MDT near the atomizer nozzle encounters the high-velocity gas sprayed from the annular slit gas outlet of the gas chamber. Subsequently, the gas–liquid two-phase fluids interact with each other. The metal melt phase deforms due to the gaseous phase, whereas the metal melt liquid column can be assumed as an ideal cylinder before the deformation. The primary break-up leads to the deformation of the metal melt liquid column. The Weber number of the liquid in the gas atomization process of the coaxial jet, i.e., the metal melt liquid column, can be expressed as follows:

$$We = \frac{\rho_g U_g^2 D_l}{\sigma}, \tag{1}$$

where ρ_g and U_g denote the density and velocity of the atomizing gas, respectively, D_l represents the diameter of the metal melt liquid column, and σ is the surface tension of the metal melt.

With a gradual increase in the Weber number, the fluctuating breakup mode mentioned in the literature can be broadly divided into the following three states:

- For a small Weber number, the liquid jet breaks up due to Rayleigh instability and exhibits two break-up modes: axisymmetric and non-axisymmetric [50].
- As the Weber number gradually increases, ribbon-like fractured segments are formed. The surface tension of the liquid affects the fracturing only in the local zones. The tip part of the ribbon-like fractured segments shrinks due to the surface tension, forming a protruding part, because the radius of curvature of such ribbon-like fractured segments is small. Subsequently, the protruding part expands under the effect of the surrounding gas. Finally, a liquid membrane is formed. This mode of break-up is referred to as the liquid membrane break-up [51].
- With a further increase in the Weber number, the size of the formed ribbon-like broken segments decreases, and the liquid breakup affords segments with a fibrous morphology.

In practical gas atomization, the primary breakup mode of the metal melt in a 2D axisymmetric atomizer is mainly determined by the local Weber number because the recirculation zone in the gas flow field is near the front end of the MDT. When the Weber number is small, the metal/alloy melt maintains a complete liquid core and continuously flows downward to the recirculation zone after flowing out of the central hole at the front end of the MDT. Subsequently, the melt interface is disturbed by the high-speed airflow owing to the Kelvin–Helmholtz (K–H) instability [52]. Such mild disturbance would present linear growth and weak nonlinear growth, which then develops into turbulent mixing through a strong nonlinear effect. In addition, the velocity inside the mixing layer changes uniformly. The velocity gradient inside the mixing layer may induce wave deformation in the shear layer, proportional to the velocity gradient.

Meiron et al. [53] thoroughly analyzed this variation process. After the fluctuation reached a certain degree, the liquid bridge between the fluctuation part and the liquid surface broke under the collaborative effect of surface tension of liquid and surface wave on the interface. Consequently, the fluctuating liquid is separated from the liquid column surface. This indicates that large droplets leave the liquid column surface, thereby leading to fluctuating breakup of the liquid column. When the Weber number is high, the metal melt follows the path of the radial outward friction exerted by the gases on its surface, after it flows out of the central hole at the front end of the

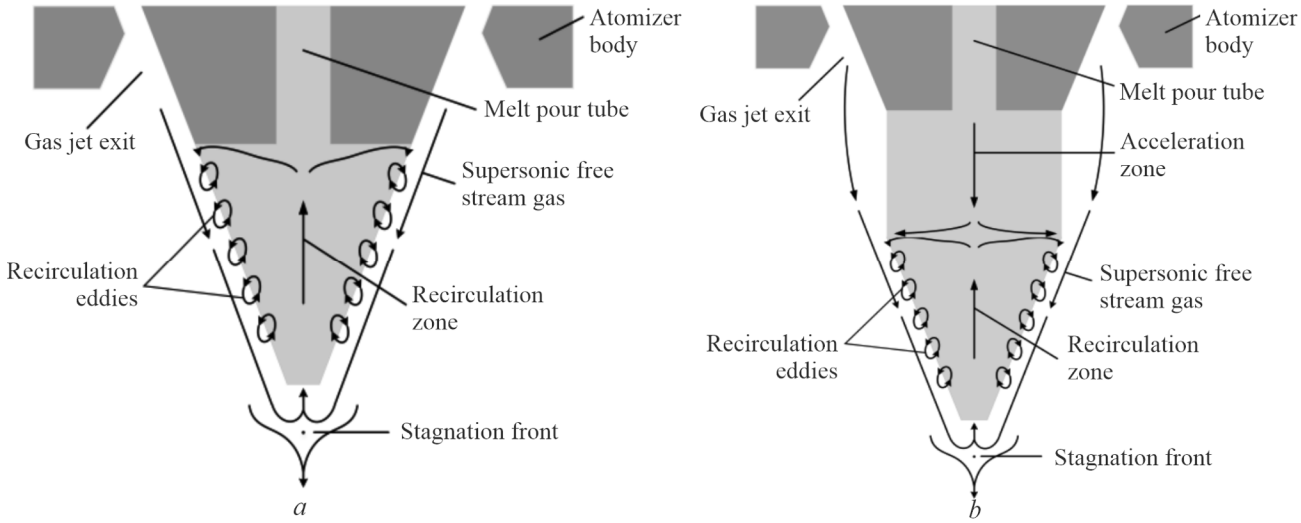

Fig. 10. Structure of the gas flow in the recirculation zone of an atomization flow field: (*a*) two-dimensional axisymmetric atomizer [59] and (*b*) vortex loop slit atomizer [58]

MDT. This is attributed to the synergy between the radial pressure gradient at the front end of the MDT and the higher velocity of the gases flowing from the front end of the MDT to the annular slit outlet than that of the melt. The liquid metal and alloy from the central hole at the front end of the MDT flow to the annular slit outlet and then directly contact the high-speed atomizing airflow. Subsequently, the high-speed atomizing airflow generates high-frequency, small-amplitude vibrations on the metal melt. Such vibrations originate from the Rayleigh–Taylor (R–T) instability [54]. These vibrations quickly spread toward the downstream region of the liquid sheet. When the wave amplitude of these vibrations penetrates the liquid sheet along its thickness, the liquid sheet breaks into small liquid droplets. This is referred to as the acting effect of short waves [55].

Mates and Settles [56] experimentally verified this phenomenon. Sheet break-up is more conducive to producing smaller atomized droplets than fluctuating break-up [57]. For the vortex loop slit atomizer, Zhang [58] analyzed the experimental and numerical simulation results of flow fields during close-coupled vortex loop slit gas atomization and observed a new gas flow field structure, which differed from that reported by Ting et al. [59], as shown in Fig. 10. However, to the best of our knowledge, there is a limited number of experimental and numerical simulation studies on the atomization mechanism of metal melts that are based on such new gas flow field structures. This necessitates advancing research on close-coupled vortex loop slit gas atomizing mechanisms.

Deformation of Droplets and Secondary Break-up. The velocity of the discrete liquid segments that are separated from the liquid column of the molten metal is less than that of the surrounding gas. As a result, large liquid segments will experience a secondary break-up due to gas-liquid interactions, which can occur by one of two mechanisms. First, under the combined action of positive pressure and friction from the gas, the droplets deform until they break up. Second, the droplets are not translational in their own right during flight. Instead, they move with some angular momentum, so that the liquid inside the droplet moves radially away from the center of the droplet due to centrifugal force. At sufficient angular velocity, the droplets will also break up. In practice, the synergy between the two mechanisms typically results in secondary droplet break-up.

In general, the droplets are regularly spherical owing to their intrinsic surface tension after the break-up and become regularly spherical powders upon solidification due to cooling. However, some metal powders exhibit a nonspherical shape, which is an intermediate morphology of the droplets during break-up. In addition, the droplets are rapidly cooled during break-up. If such droplets solidify before complete break-up, their intermediate morphology is preserved; the intermediate process during droplet break-up can be interpreted from this morphology. The formation of powders with the abovementioned morphology substantiates the initial conclusion drawn by Pilch and Erdman [60]—the droplets are subjected to fluctuating break-up at a small Weber number.

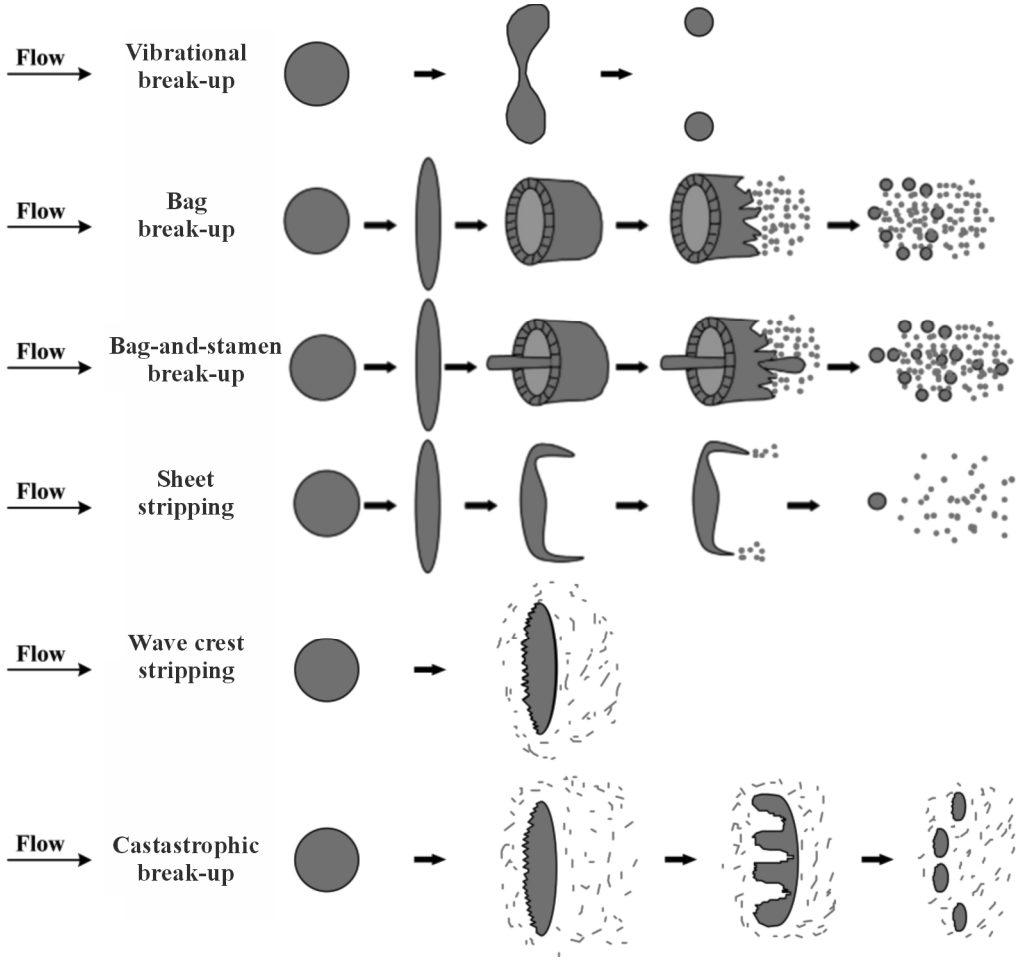

Fig. 11. Animation of the break-up mechanisms: these mechanisms qualitatively describe the break-up of water droplets [60]

Pilch and Erdman summarized the following five droplet break-up modes in a straight flow field under different Weber numbers [60], as shown in Fig. 11:

(1) Vibrational break-up ($0 < We \leq 12$);

(2) Bag break-up ($12 < We \leq 50$);

(3) Bag-and-stamen break-up ($50 < We \leq 100$);

(4) Sheet stripping ($100 < We \leq 350$);

(5) Wave crest stripping followed by catastrophic break-up ($We > 350$).

To determine the break-up mechanisms of a droplet in a swirling flow field, Kirar et al. [47] used shadowgraphy and PIV and analyzed the dynamics of interaction of an ethanol droplet with a swirling airflow in an orthogonal arrangement, experimentally and theoretically. Their results revealed a new breakup mode, termed retracting bag break-up, under the swirling flow condition, as shown in Fig. 12. Herein, as the droplet deforms to a disk shape owing to its interaction with the airflow, it experiences a differential flow field because of the presence of the wake of the vanes and the central recirculation zone under swirling flow conditions, unlike the conventional break-up modes under straight flow conditions. Consequently, the bag expands in the upper half of the droplet but contracts in the lower half, thereby fragmenting the bag, similar to the bag retreating.

In contrast to the straight flow, the swirling flow promotes the R–T instability, increasing the stretching factor in the droplet deformation process and forming many fingers on the droplet surface (as shown in Fig. 13). A modified theoretical analysis was proposed based on the R–T instability mechanism for swirling flows and was

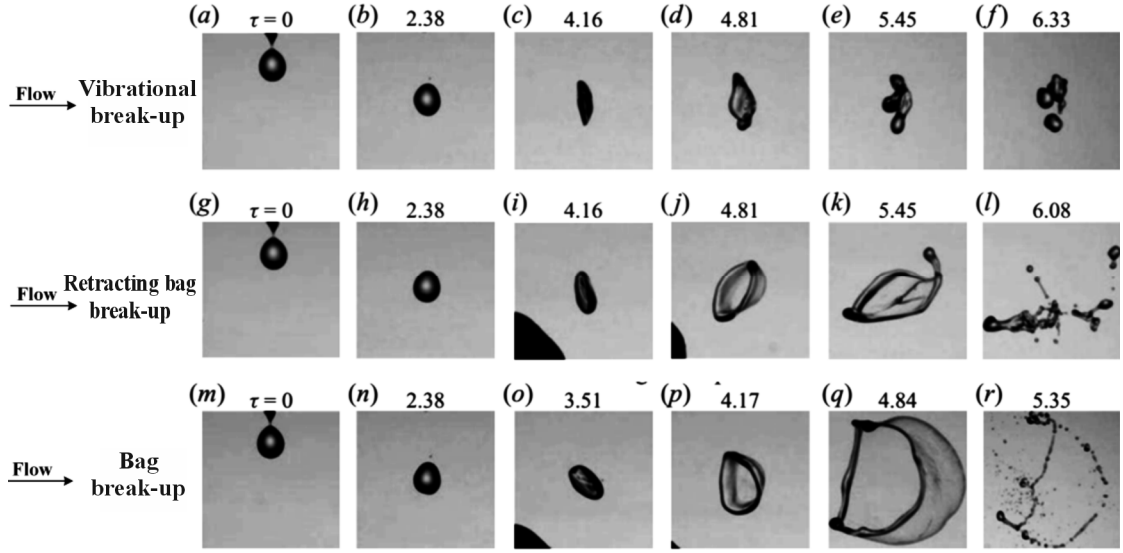

Fig. 12. Temporal evolution of the break-up dynamics for different values of swirl number, *Sw*: (*a–f*) *Sw* = 0 (no swirl), (*g–l*) *Sw* = 0.47 (low swirl strength), and (*m–r*) *Sw* = 0.82 (high swirl strength) [47]

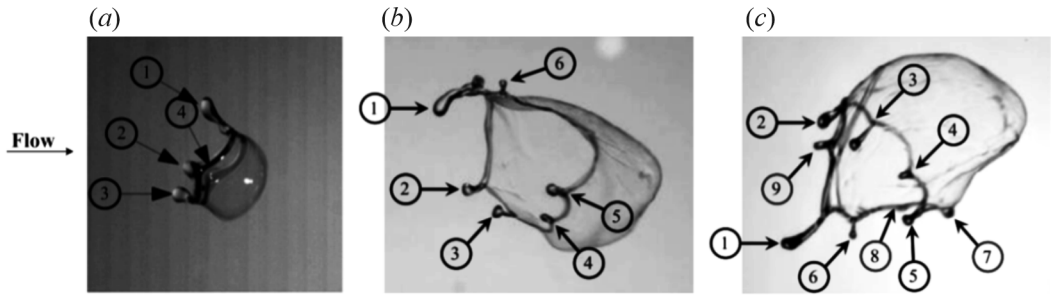

Fig. 13. Computation of the number of fingers using the (*a*) front view (12 < *We* < 16, *Sw* = 0, and $\bar{z}_d = 0$) [61], (*b*) front view (*x–y*) (*We* = 14.54, *Sw* = 0.82, $\bar{x}_d = 0.01$, $\bar{y}_d = 0.89$, and $\bar{z}_d = -0.13$) [47], and (*c*) top view (*x–z*) (*We* = 14.54, *Sw* = 0.82, $\bar{x}_d = 0.01$, $\bar{y}_d = = 0.89$, and $\bar{z}_d = -0.13$) [47]

verified experimentally. However, there are limited experimental and numerical simulation studies on the break-up mechanisms of a droplet in a high-speed swirling flow field, to the best of our knowledge. This necessitates research progress in the break-up mechanisms of a droplet in a high-speed swirling flow field.

NUMERICAL SIMULATION STUDIES ON GAS ATOMIZATION FLOW FIELD OF THE ATOMIZER

During gas-atomization-based powder preparation, the high-temperature metal melts undergo complex physical and chemical reactions in a closed atomization chamber filled with a protective gas and finally form a solid powder. In this process, the flow of the metal melt, changes in the gas properties, melt break-up, and cooling and condensation of molten droplets usually occur under high-temperature, high-pressure, and extreme gas-liquid impact conditions, potentially accompanied by instantaneous changes in the melt properties. Therefore, this poses challenges to real-time studies on the flow behaviors of metal melt in the atomization system, changes in gas properties, melt break-up, and evolution of the molten droplet morphologies and states during the break-up. Moreover, there is no existing theory to guide studies on atomization mechanisms.

Since the rapid development of computers and numerical computing technology in the 1990s, computational fluid dynamics (CFD) has been globally used by researchers for studying changes in the gas flow

field characteristics of atomizers [59]. Several numerical simulation studies have determined the microstructure of the atomizer gas flow field and the influence of atomization parameters on the atomizer gas flow field characteristics. The results provide visual and theoretical clues for predicting normal atomizer operation and melt break-up.

In 1996, Mi et al. [62] simulated the influence of the atomizing gas pressure on the gas flow field characteristics in an annular slit HPGA nozzle using the PHOENICS software. The simulation results demonstrated the existence of a recirculation zone atop the MDT. In addition, a radial pressure gradient is prevalent, which gradually decreases in the radial direction, and the maximum static pressure occurs atop the central hole of the MDT. Upon increasing the atomizing gas pressure to 4 MPa, a positive shock-wave structure occurs in the flow field. Simultaneously, a Mach disk is formed along the central line of the flow field. With an increase in the atomizing gas pressure, the Mach disk moves farther from the top of the MDT along the central line of the flow field, and the intensity increases gradually. In 1997, Liu and Dax [63] simulated the influence of an unrestricted nozzle structure on the gas flow field by solving the Navier–Stokes equation and proposed that the flow field in the recirculation zone could be changed by adding a secondary airflow.

In 1998, Yu and Anderson [64] simulated and analyzed the changes in gas velocity produced by four nozzles with different geometric structures, using the RAMPANT software. They reported that the geometric structure of the nozzle obtained using the characteristic method has the lowest loss of gas energy. In the same year, Espina and Piomelli [65] simulated the effects of the atomizing gas pressure and temperature on the gas flow field using the NPARC software and pointed out that the separation of the atomizing gas from the external top wall of the MDT is the major cause of condensation of the metal melt.

In 1998, Chen and Yin [66] and Chen [67] studied the geometric structure and working mechanism of a vortex loop slit atomizer and pointed out that an increase in the ratio between the inner cavity and annular slit gas outlet diameters and a decrease in the annular slit width is conducive to increasing the resultant velocity when the atomizing medium is sprayed from the annular slit gas outlet of the nozzle, thereby increasing the atomization efficiency. The fluid atomizing medium does not focus at one point after being sprayed from the vortex loop slit atomizer; it forms a hollow double cone. To prevent choking, the extension concentrate of the leakage pipe should be designed such that the upper negative pressure zone of the opening of the hollow double cone is theoretically closed. In the same year, Chen [68] analyzed the working characteristics of a vortex loop slit atomizer from a fluid-mechanics perspective and pointed out that the working efficiency of the atomizer can be influenced by the unreasonable structural size, relatively high roughness of the internal wall, and low concentricity of the annular slit. An atomizer with excellent performance should decrease the energy loss of the atomizing media when the media pass through the atomizer, and should maintain a relatively high linear velocity of the atomizing media while spraying from the loop slit outlet.

In 2002, Sun et al. [69] simulated the influence of the protrusion length of the MDT on the gas flow in a restricted loop slit atomizer using the CFD-CAE+ software. The results demonstrated that the gas flow velocity in the atomizer chamber changes with the axial and radial positions. The gas flow velocity decreases with an increase in the distance of the gas from the front end of the MDT. When the protrusion length of the MDT is less than 1 mm, the gas flows inversely in the MDT, which may cause an inverse flow of the metal melt. When the protrusion length of the MDT is greater than 1 mm, the gas in the MDT flows downward, inducing a pumping effect on the metal melt, which is conducive to spraying.

In 2004, Ting and Anderson [59] conducted a simulation study on the gas flow field of a loop slit HPGA nozzle using the RAMPANT software. They observed that the atomizing gas pressure exhibits nonlinearity with the gas flow field structure. An increase in the atomizing gas pressure increases the atomizing gas velocity, thereby narrowing and lengthening the recirculation zone. After the atomizing gas pressure exceeds the critical value, the flow field in the recirculation zone changes from the open-wake state to the closed-wake state. In the open-wake state, there is only one stagnation point with an atomizing gas velocity of 0 m/s in the recirculation zone. In the closed-wake state, there are two stagnation points with atomizing gas velocities of 0 m/s in the recirculation zone. Moreover, the recirculation zone compresses longitudinally and then stretches transversely.

In 2005, Fritsching [70] discussed the roles of gas flow in the atomizer vicinity of a twin-fluid atomizer, primary and secondary fragmentation processes, and multiphase flow in the spray, demonstrating the production of fibrous or spherical particles by melt atomization. The experimental results showed that for constant atomizing gas pressures, the powder-to-fiber ratio increases with increasing gas temperature and decreasing gas mass flow rate or gas-to-melt mass flow rate. In addition, at a constant gas temperature, the mass median diameter of the powder particles decreases with increasing gas pressure.

In 2007, Chen [71] simulated the influence of the geometric structural parameters of a loop slit HPGA nozzle on the gas flow field structure using the FLUENT software. He found out that the critical atomizing gas pressure (P_c) for the gas flow field structure changes from the open-wake state to the closed-wake state and is sensitive to changes in the protrusion length of the MDT. Moreover, P_c is negatively correlated with the protrusion length of the MDT.

In 2008, Zeoli and Gu [72] used the commercial CFD software, FLUENT, to calculate a single-phase gas jet. According to the calculated results, many shockwaves are present in the supersonic jet velocity field. This finding is consistent with the phenomenon observed by Ting et al. [73]. When a high-pressure gas enters the nozzle, swelling wave beams are produced successively, thereby increasing the gas velocity. Subsequently, the swelling wave beams are reflected by the external wall surface of the MDT, and an oblique shockwave is formed in the nozzle. At the nozzle outlet, the gas passes through a series of Prandtl–Meyer swelling waves and recompression shocks, attaining equilibrium with the internal pressure of the atomization chamber. Moreover, the sound velocity layer separates the outer part of the jet region from the jet core region. In this sound velocity layer, the gas velocity is lower than that in the supersonic jet core region. Hence, the high-speed gas sprayed from the nozzle outlet continuously impacts the sound velocity layer and then enters the external low-speed jet region. Consequently, an external flow field is formed out of the jet core. However, the gas in the external flow field cannot easily penetrate the sound velocity layer to enter the supersonic jet core region.

In 2008, Jeyakumar et al. [74] performed a 2D simulation of the atomizing gas flow field in a gas collection chamber and at the outlet of a contraction gas flow nozzle using the FLUENT software and discussed the influence of the protrusion length of the MDT on the aspiration pressure. They reported that the density, pressure, and static temperature of the atomizing gas are not related to the geometric structure of the nozzle. When the protrusion length of the MDT is increased from 0 to 2 mm, the aspiration pressure decreases gradually and reaches a valley at 2 mm. Upon increasing the protrusion length of the MDT to 3 mm, the aspiration pressure gradually increases. In the same year, Tong and Browne [75] conducted a direct numerical simulation study of the dynamic interactions between Raney Ni–Al intermetallic melt and argon gas at the start of atomization, near the nozzle of a close-coupled gas atomizer using a front-tracking formulation. According to the calculated results, gas recirculation is observed as a strong feedback of the melt to the gas. However, the effects of gas on the melt stream are different before and after the melt stream disconnection, proving the influence of the feedback. Furthermore, owing to the existence of the melt, the mechanism of stagnation point formation differs from that in the gas-only case.

In 2009, Allimant et al. [76] studied the influence of the pressure and velocity of the atomizing gas and the pressure in the atomization chamber on the gas flow field in a laminar gas atomization nozzle using the FLUENT software. In the same year, Zhao et al. [77] simulated the influence of atomizing gas pressure in a supersonic gas atomization nozzle and the protrusion length of the MDT on the gas flow field using the FLUENT software. The results showed the prevalence of a series of alternating swelling wave beams and compressive waves in the gas flow field under the action of aerodynamics. An increase in the protrusion length of the MDT increases the intensity of the Mach disk; however, the aspiration pressure decreases gradually, ultimately leading to negative pressures. Positional changes in the stagnation point on the centerline of the flow field and Mach disk alter the velocity and static temperature of the atomizing gas in the gas flow field.

In 2010, Ouyang et al. [78] simulated the open-wake and closed-wake structural characteristics in the gas flow field of a close-coupled straight annular slit atomized nozzle and the abrupt change behaviors using the FLUENT software. Additionally, the effects of the atomizing medium type and major geometric structural parameters of the nozzle—spraying apex angle, protrusion length and tip diameter of the MDT, and annular slit

width—on the P_c were studied. The results demonstrated that the atomizing gas pressure (P) is slightly higher than the P_c, the recirculation zone is rapidly intercepted by the Mach disk, and the flow-field structure abruptly changes from the open-wake state to the closed-wake state. Moreover, the aspiration pressure (P_a) at the front end of the MDT decreases sharply. That is, the aspiration pressure difference before and after the abrupt change (ΔP_a) is approximately 30 kPa. The type of atomizing medium and major geometric structural parameters of the nozzle exert a significant influence on the P_c, but no influence on the ΔP_a.

In 2011, Aydin and Ünal [79] simulated the influence of the atomizing gas pressure and geometric structure of nozzles on the atomizing gas velocity at the outlet of the nozzle using computers. They found out that the atomizing gas velocity does not monotonously vary with an increase in the atomizing gas pressure. When the atomizing gas pressure is 2.7 MPa, a maximum atomizing gas velocity of 663 m/s is achieved. When the atomizing gas pressure is 1.0 MPa, a minimum atomizing gas velocity of 631 m/s is obtained. An optimum geometric structure of the nozzle can result in a high atomizing gas velocity under the same gas–liquid mass flow rate, thereby increasing the atomization efficiency. In the same year, Zeoli et al. [80] simulated the flow field structures of an annular slit atomizer, swirling gas atomizer, and inner-jet atomizer using the FLUENT software, by combining the volume of fluid (VOF) algorithm and Reynolds stress model (RSM). According to the comparison of the simulation results, the inner-jet atomizer can effectively improve the performance of the atomized powder, whereas the swirling gas atomizer cannot. Liu [81] analyzed the design parameters of a close-coupled vortex loop slit atomizer from the viewpoint of fluid mechanics. He proposed a qualitative analysis and quantitative description of the design parameters of the close-coupled vortex loop slit atomizer. The mathematical expressions for the loop slit area and maximum size of the vortex loop slit atomizer and the diameters of the fluid medium delivery tubes without turbulence were given, from which the mathematical expression for the atomizing apex angle was established using design computations. The importance of ensuring the concentricity of the vortex loop slit atomizer was discussed.

In 2012, Zhao [82] and Zhao et al. [83] performed a numerical simulation of the gas flow field structure for an increase in the angle of intersection at the atomizer gas outlet from 5° to 65°, using the k–ε and RSM models. They observed that the annular velocity peak occurs at a position below the MDT and near the atomizer. With an increase in the angle of intersection at the atomizer gas outlet, the position for integrating annular velocity peaks becomes farther from the front end of the MDT. Moreover, the scattering angle of the main part of the gas spray increased continuously. According to the comparison of the experimental results, the RSM model is more accurate than the k–ε model. A close-coupled atomizer with an angle of intersection at the atomizer gas outlet within this interval can produce an aspiration pressure lower than the environmental pressure at the front end of the MDT. Additionally, the atomizer with an angle of intersection of 55° at the atomizer gas outlet produces the highest aspiration pressure.

In the same year, Zhao et al. [84] investigated the primary atomization process in a close-coupled atomizer by combining the traditional fluctuation theory with the VOF algorithm. They discovered that during the primary atomization in this close-coupled atomizer, the metal melt breaks via two modes: fluctuating break-up and liquid membrane break-up. They determined the range of the Weber number for mutual transformation between the two breakup modes as 130.1–160.9. Zeoli et al. [85] numerically investigated the unstable features of a hot liquid metal entering an atomization tower using a 3D, turbulent, unstable simulation using the VOF method and the large-eddy simulation turbulence-capturing technique. The initial results demonstrated that a gas-only flow simulation is not adequate to represent the fluid mechanics, owing to the significant changes caused by the melt. The flow pattern for the primary break-up of the liquid melt column is not 2D axisymmetric; a 3D model is necessary to study the unstable gas–melt agitation and pinch-off process. The computational model predicted three modes for close-coupled atomizers, namely, nozzle filming, mixed filming and pinch-off, and no-filming, which are determined by the gas-to-melt ratio.

In 2013, Motaman et al. [86] studied the effect of the gas flow angle of the nozzle on the backflow at the outer wall surface along the protrusion length of the MDT in a close-coupled gas atomizer. They investigated the atomization performance of a convergent–divergent (C–D) discrete gas jet die at five different atomization gas pressures ranging from 1 to 5 MPa, with different gas exit jet distances of 1.65, 1.6, 1.55, 1.5, 1.45, and 1.40 mm

from the external wall of the melt nozzle. Additionally, four melt nozzles with varying gas jet mismatch angles of 0°, 3°, 5°, and 7°, relative to the melt nozzle external wall, were used.

In 2014, Fu [87] conducted a simulation study of the influence of four atomizing media—argon, air, nitrogen, and helium—on the gas atomization flow field using the FLUENT software. They demonstrated that the maximum velocities of argon, air, nitrogen, and helium in the single-phase gas atomization flow field are 535.19, 705.74, 711.22, and 1074.22 m/s, respectively. The static temperature and velocity distributions in the single-phase gas atomization flow field under the four atomizing media were consistent. The lowest static temperatures are 24.96, 52.59, 60.75, and 20.43 K, respectively. Under the same pressure conditions of the atomizing media, the aspiration pressure intensities atop the MDT are –90.26, –75.49, –71.25, and –50.85 kPa, respectively. Moreover, the static pressure intensities in the radial distribution atop the MDT have corresponding pressure gradients.

In 2015, Motaman et al. [88] investigated the single-phase gas flow behavior of a close-coupled gas atomizer using four different melt nozzle tip designs and two types of gas die. Both the melt nozzle tip design and the type of die significantly influence the wake closure pressure (WCP), and the C–D gas die yields significantly high WCPs.

In 2016, Wang et al. [89] numerically simulated the primary atomization process of an airflow-atomized metal melt in the form of a tornado using the FLUENT software to explore the primary atomization process of the metal melt under the effect of a swirling airflow field. The results showed that a liquid membrane was more easily formed in the metal melt due to the vortex in the swirling airflow field than that in the non-swirling airflow field, accompanied by a higher utilization rate of the gas. For the same mass flow rate (0.01 kg/s) of the metal melt, the metal melt facilitates a sudden change from the microfountain break-up mode into the classical umbrella-like liquid membrane break-up mode at a critical gas mass flow rate of 0.0038 kg/s.

In 2017, Ma and Zhang [90] carried out a numerical simulation study on the flowing process in a close-coupled vortex loop slit atomizer and jet flow field characteristics after airflow was sprayed from the loop slit gas outlet of the atomizer by using the FLUENT software. They found that there were vortexes of gas flow in the atomizer. The flow field of the jet from the loop slit gas outlet of the atomizer exhibits a hollow opposite gas-coning morphology with a rotation. The jet flow rate decreased gradually along the spraying direction, while the jet width increased gradually. In the same year, Schwenck et al. [91] designed different nozzles with conventional and convergent−divergent annular geometry based on fluid-flow calculations. They found that this novel configuration is capable of operating stably at low pressures of 0.8 MPa and above. Beyond that, the unwanted effects of lick-back were avoided. Moreover, Li and Fritsching [92] implemented a detailed study of the mutual coupling process of break-up, cooling, and solidification of metal melt in the vortex atomizer and provided research directions for exploring the primary and secondary break-up processes of metal melt in the vortex atomizer.

In 2018, Kaiser et al. [93] conducted a numerical simulation study of the high-pressure gas atomization process to determine the existence of efficient paths to optimize the gas–melt interactions and to elucidate the possible effects of the shockwaves. The results revealed the existence of more efficient paths for more optimum utilization of the gas kinetic energy, and that shock waves are detrimental to producing powders with smaller particles. In the same year, Kayali and Ünal [94] investigated the interaction between the liquid metal and atomizing gas via the VOF method using the ANSYS/FLUENT software. The analyses demonstrated that the VOF method yields excellent results in terms of predicting the flow dynamics, atomization mechanism, and particle size and distribution for gas atomization.

In 2019, Arachchilage et al. [95] investigated the effects of atomization gas pressure in an annular slit and the close-coupled gas atomizer on the gas atomization process of molten aluminum and droplet size distribution by combining the VOF model with the geometric reconstruction method in the OpenFOAM software. The results demonstrated that the atomization rate increases with increasing gas pressure. The effectiveness of the atomization process increases with increasing gas pressure. In the same year, Hernandez et al. [96] compared high-resolution 3D simulations employing a five-equation compressible flow model coupled with the VOF method and experiments for liquids with Weber numbers ranging between 1 and 30 and Reynolds numbers less than 10,000. They explored the predicting capabilities and limitations of the compressible multiphase mixture numerical model.

In 2020, Beckers et al. [97] examined the influence of the gas flow pattern on the particle shape and circularity in the powder production of metal particles for AM by spraying, using the CFD Solver from COMSOL Multiphysics. The effect of coaxial auxiliary gas flow in the spray chamber on the flow structure was analyzed. Velocity data from the experimental setup were used to validate the gas flow. The gas flow from the 3D tangential atomizer nozzle spirals downwards along the walls of the spray chamber, and the use of an additional coaxial gas leads to an increase in the circularity of the particles of up to 10% for the relevant particle sizes. The results of the particle measurements indicate the presence of many small particles in the powder, with a shift to smaller particles when coaxial gas is used. The coaxial gas reduces the average particle size by allowing some small particles to adhere to the primary particles and form satellite powders.

In 2021, Zhang et al. [98] and Zhang et al. [99] simulated the effects of atomizing gas pressure in a close-coupled vortex loop slit atomizer, annular slit width, and protrusion length of the MDT on the gas atomization flow field using the FLUENT software. The annular slit width impacts the gas flow field of the atomizer more severely than the atomizing gas pressure and protrusion length of the MDT. The differences in the location of the stagnation point and stagnation pressure in the gas flow field of atomizers are major causes for the variations in the volume of the recirculation zone and the aspiration pressure intensity at the front end of the MDT. In the same year, Zhang et al. [100] investigated the effects of various operating conditions on the performance of a high-pressure-gas close-coupled atomizer via experiments and computer simulations. The results demonstrated that the performance of the atomizer is determined by the interaction of three forces on the surface of the nozzle: gravity, suction, and gas shear force. The shear force and gravity play a dominant role in determining the melt flow rate. Moreover, an increase in the atomizing gas pressure leads to a finer powder size distribution but lower powder throughput.

Liu et al. [101] numerically simulated the flow mechanism inside the MDT of a metal melt during the gas-atomization-based powder preparation process based on the VOF interface-capturing algorithm and the shear–stress transport k–ω turbulence model. The results indicated that the flow resistance encountered by the metal melt in the MDT is aggravated by a decrease in the inner diameter of the MDT. As the inner diameter of the MDT is reduced to 1 mm, the resistance of the metal melt flowing in the MDT reaches an order of magnitude of 10^2 kPa. When the inner diameter of the MDT is reduced from 4 to 2 mm, the yield rate of fine powder (<150 μm) by gas atomization considerably in creases from 54.7 to 94.2%. The surface quality of the powders has improved upon using an MDT with a smaller inner diameter. Moreover, Luo et al. [102] simulated the complex gas atomization (GA) process to produce metal powders using the ANSYS FLUENT software. They combined the VOF model with a dynamic adaptive mesh and a discrete phase model, wherein the gas atomization details include the break-up of the continuous liquid and droplets, and conducted an experimental verification. The simulation results showed that the K–H instability in the primary atomization and the membranous droplet break-up and closure in the secondary atomization result in the formation of a hollow powder; the satellite powder is formed because of collisions between the large and small droplets with different velocities. Furthermore, an irregular powder is produced when the drag force is not sufficient to separate the droplets, resulting in their deformation.

In summary, studies on atomizers mainly involve the geometric structures, gas flow field characteristics, and atomizing performance of the atomizer. Because only the atomizing process with a gas flow is closely related to the practical atomizing process, many studies are based on the influence of the geometric structural parameters of the atomizer and atomizing technological parameters on the gas flow field characteristics, with the aim of determining the designs of atomizers.

Researchers have analyzed the effects of the geometric structural parameters of the atomizer and atomizing technological parameters on the recirculation zone size and shape, aspiration pressure intensity, and atomizing gas velocity in the gas flow field. However, further studies are needed to formulate a complete set of design codes for atomizers. Most researchers have focused on the geometric nozzle structure of 2D axisymmetric atomizers, gas flow field characteristics of the nozzle, and atomizing performance. However, to the best of our knowledge, there are limited in-depth studies on the geometric structure, gas flow field characteristics, and atomizing performance of 3D vortex loop slit atomizers. Hence, the atomization characteristics and mechanisms of vortex loop slit atomizers need to be understood further, as shown in Fig. 14.

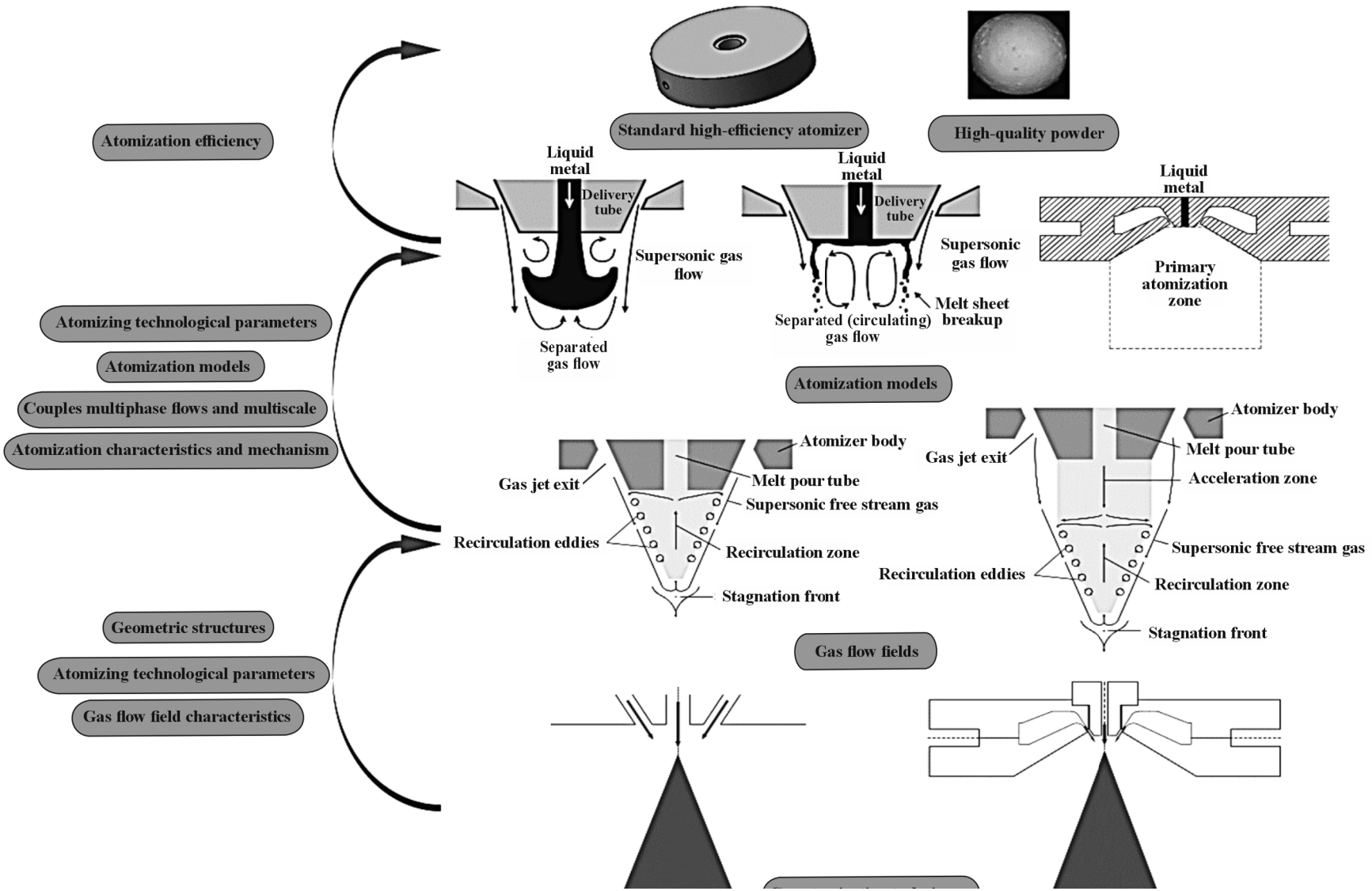

Fig. 14. Efficiency challenges between gas atomization process and high-quality powders

CONCLUSIONS AND OUTLOOK

Although researchers have studied the atomization characteristics and mechanisms of the close-coupled atomizer for more than 30 years [15], there is no consensus on the atomization mechanism, owing to the complex and unstable characteristics of the atomization process. Designing a close-coupled atomizer with significant atomizing characteristics remains challenging. Through theoretical analysis, numerical calculations, and experimental tests, the performance of close-coupled atomizers should be continuously improved. Experimental measurement methods, breakup mechanisms of metal melts, and atomization models must be established for powder preparation based on close-coupled gas atomizers.

Based on the existing research, this paper demonstrates the impending challenges in determining the experimental test method and studies the atomization characteristics and mechanisms of the close-coupled vortex loop slit atomizer. The summary is as follows:

1) The influencing mechanisms of the included angle of the annular slit gas outlet, inner diameter of the central hole of the MDT, and degree of superheating of the metal melt in the single-phase gas flow field characteristics and atomization performances of the close-coupled vortex loop slit atomizer should be studied.

2) The existing experimental testing technologies should be optimized to measure the flow fields near the front end of the MDT and on the transverse section during the gas atomization of the close-coupled vortex loop slit atomizer. This can deepen our understanding of the atomization characteristics and mechanisms of the close-coupled vortex loop slit atomizer.

3) Carry out the experimental and numerical simulation studies on the primary atomization process of the metal melt in a swirling flow field, such as influences of swirling flow field structure on the atomization process of the metal melt, influences of the metal melt on swirling flow field structure, classification of atomization modes of the metal melt in a swirling flow field, intrinsic physical mechanisms responsible for atomization of the metal melt in a swirling flow field, and influences of phase change on atomization process of the metal melt [103], etc.

4) Experimental and numerical simulation studies on the process of deformation and break-up of a drop of molten metal in a field of high-speed turbulent flow are required.

5) Key factors influencing the breakup mode transformation of the metal melt in the gas flow field of the close-coupled vortex loop slit atomizer should be analyzed, based on which the sheet-forming and break-up mechanisms of the metal melt in the swirling flow field can be elaborated further.

ARTICLE-LEVEL DECLARATIONS

Conflict of Interest. The authors declare that they have no known competing financial interests or personal relationships that could have appeared to influence the work reported in this paper.

Funding. This work was financially supported by the National Natural Science Foundation of China (Nos. 11532015 and U1738119) and the Priority Academic Program Development of Jiangsu Higher Education Institutions (PAPD), which are gratefully acknowledged.

Author Contributions. Min Zhang designed the research and wrote the first draft of the manuscript. Zhaoming Zhang and Qiusheng Liu helped organize the manuscript. Min Zhang and Qiusheng Liu revised and edited the final version.

Data Availability. Data will be made available on request.

REFERENCES

1. G. Dowson, *Powder Metallurgy: The Process and its Products*, Edition 1, Springer Netherlands, New Manufacturing Processes and Materials Series (1990).
2. R. German, *Powder Metallurgy Science*, Metal Powder Industry Federation, Princeton (1994).
3. A. Lawley, *Atomization, the Production of Metal Powder,* Metal Powder Industry Federation, Princeton (1992).
4. Y.F. Mu, *Study on Process Optimization of Gas Atomization for Preparation of Fine Metal Powders*, PhD, Central Southern University, Changsha, Hunan, China (1997).

5. John K. Beddow, *The Production of Metal Powders by Atomization*, John Wiley & Sons Ltd, Heyden (1978).
6. M. Xia, P. Wang, X.H. Zhang, and C.C. Ge, "Computational fluid dynamic investigation of the primary and secondary atomization of the free-fall atomizer in electrode induction melting gas atomization process. *Acta Phys. Sin*., **67**, 41–51 (2018).
7. E. Klar and W.M. Shafer, *Powder Metallurgy for High Performance Applications*, Syracuse University Press, New York (1972).
8. H.W. Ouyang, X. Chen, W.T. Yu, and B.Y. Huang, "Progress and prospect on the gas atomization," *Powder Metall. Technol.*, **25**, No. 1, 53–58 (2007).
9. O.S. Nichiporenko and Y.I. Naida, "Heat exchange between metal particles and gas in the atomization process," *Powder Metall. Met. Ceram.*, **7**, 509–512 (1968).
10. J.J. Dunkley, "Liquid atomization," *Powder Metall*., **32**, 96–97 (1989).
11. N.J. Grant, "A review of various atomization processes," *Phys. Mech. Metall.*, **35**, 20 (1983).
12. R. Rutharde, "Novel aspects for high quality metal powders equipment*," Int. J. Powder Metall.*, **13**,175–179 (1981).
13. A. Walz, *Metal Powders and a Process for the Production Thereof*, Pat. 4,534,917 U.S., 1985–08–13.
14. I.E. Anderson, "Boost in atomizer pressure shaves powder-particle size," *Adv. Mater. Proc.*, **140**, 30–32. (1991).
15. S.A. Miller, "Close-coupled gas atomization of metal alloys," in: W.A. Kaysser, W.J. Huppmann (Eds.). *Future of Powder Metallurgy*, *P/M '86*: Proceedings of the 1986 International Powder Metallurgy Conference (Dusseldorf, 1986), Vol. 2, Verlag Schmid GmbH, Freiburg (1986).
16. A. Ünal, M.J. Naylor, and H.B. McShane, "Modelling of metal powder production using a wax atomizer," *Powder Metall*., **33**, 260–268 (1990).
17. B. Hopkins, "Close-coupled gas atomization comes of age," *Met. Powder Rep.*, **49**, 34–38 (1994).
18. G. Schulz, "NANOVAL process offers fine powder benefits," *Met. Powder Rep.*, **51**, 30–33 (1996).
19. J.X. Xu, C.Y. Chen, L.Y. Shen, W.D. Xuan, X.G. Li, S.S. Shuai, X. Li, T. Hu, C.J. Li, J.B. Yu, J. Wang, and Z.M. Ren, "Atomization mechanism and powder morphology in laminar flow gas atomization," *Acta Phys. Sin.*, **70**,140201 (2021).
20. J.T. Strauss, "Hotter gas increases atomization efficiency," *Met. Powder Rep.*, **54**, 24–28 (1999).
21. S. Hussain, C. Cui, L. He, L. Madler, and V. Uhlenwinkel, "Effect of hot gas atomization on spray forming of steel tubes using a close-coupled datomizer (CCA)," *J. Mater. Proc. Technol.*, **282**, 116677 (2020).
22. P. Wang, J. Li, X. Wang, B.R. Du, S.Y. Shen, X.Y. Ge, and M.H. Wang, "Impact mechanism of gas temperature in metal powder production via gas atomization," *Chin. Phys. B*, **30**, 1–15 (2021).
23. G. Schulz, "Taking the pressure out of atomization," *Met. Powder Rep.*, **57**, 23–25 (2002).
24. P. McGuinness, W. Drenckhan, and D. Weaire, "The optimal tap: Three-dimensional nozzle design," *J. Phys. D Appl. Phys.*, **38**, 3382–3386 (2005).
25. C. Czisch and U. Fritsching, "Atomizer design for viscous-melt atomization," *Mater. Sci. Eng. A*, **477**, 21−25 (2008).
26. W.S. Prashanth, S.L. Thotarath, S. Sarkar, T.N.C. Anand, and S. Bakshi, "Experimental investigation on the effect of melt delivery tube position on liquid metal atomization," *Adv. Powder Technol.*, **32**, 693–701 (2021).
27. D.Y. Choi, J.W. Byun, and H.M. Park, "Analysis of liquid column atomization by annular dual-nozzle gas jet flow," *J. Fluid Mech.*, **943**, A25 (2022).
28. M. Zhang, *Study on the Gas Flow Field in Close-Coupled Vortical Loop Slit Atomizer and the Atomization Mechanism*, PhD, Nanjing University of Aeronautics and Astronautics, Nanjing, China (2021).
29. J. He, S.Z. Ma, X.G. Zhang, X.Q. Gai, H.H. Chen, and K.C. Zhang, "Research progress and prospects of metal powder preparation technique for additive manufacturing, *Mater. Mech. Eng.*, **44**, 46–58 (2020).

30. T.L. Zhang and C.-T. Liu, “Design of titanium alloys by additive manufacturing: A critical review, *Adv. Powder Mater.*, **1**, 100014 (2022).
31. J.L. Zhang, W.H. Yuan, B. Song, S. Yin, X.B. Wang, and Q.S. Wei, “Towards understanding metallurgical defect formation of selective laser melted wrought aluminum alloys, *Adv. Powder Mater.*, **1**, 100035 (2022).
32. R.F. Xu, Z.W. Geng, Y.Y. Wu, C. Chen, M. Ni, D. Li, T.M. Zhang, H.T. Huang, F. Liu, R.D. Li, and K.C. Zhou, “Microstructure and mechanical properties of in-situ oxide-dispersion-strengthened NiCrFeY alloy produced by laser powder bed fusion,” *Adv. Powder Mater.*, **1**, 100056 (2022).
33. W.H. Wu, T. Wang, and D. Fang, “Research progress on main preparation technologies of spherical metal powder for additive manufacturing,” *Mater. Mech. Eng.*, **45**, 76−83 (2021).
34. X.X. Fu, Y.X. Lin, X.J. Yue, M. Xun, B. Hur, and X.Z. Yue, “A review of additive manufacturing (3D printing) in aerospace: Technology, materials, applications, and challenges,” in: Dalai Tang, Junpei Zhong, Dalin Zhou (Eds.), Mobile Wireless Middleware, Operating Systems and Applications: 10th International Conference on Mobile Wireless Middleware, Operating Systems and Applications (MOBILWARE 2021), Springer Science and Business Media Deutschland GmbH (2022), pp. 73−98.
35. X.G. Li, C. Liu, and Q. Zhu, “Research progress on gas atomization technology for preparation of feedstock powder used in metal additive manufacturing, *Aeronaut. Manuf. Technol.*, **62**, 22–34 (2019).
36. A. Mostafaei, A.M. Elliott, J.E. Barnes, F.Z. Li, W.D. Tan, C.L. Cramer, P. Nandwana, and M Chmielus, Binder jet 3D printing—Process parameters, materials, properties, modeling, and challenges,” *Prog. Mater. Sci.*, **119**, 100707 (2021).
37. A.H. Lefebvre and V.G. McDonell, *Atomization and Sprays,* CRC Press, Boca Raton (2017).
38. X.H. Gan, *Aero Gas Turbine Engine Fuel Nozzle Technology*, National Defense Industry Press, Beijing (2006).
39. W.D. Bachalo, “Experimental methods in multiphase flows,” *Int. J. Multiphas. Flow*, **20**, 261−295 (1994).
40. F. Durst and M. Zare, “Laser Doppler measurements in two-phase flows, in: *The Accuracy of Flow Measurements by Laser Doppler Methods*: Proceedings LDA Symposium, Copenhagen, Denmark (1975), pp. 403−429.
41. W.D. Bachalo, “Spray diagnostics for the twenty-first century,” *Atomization Spray*, **10**, 439−474 (2002).
42. F. Durst, G. Brenn, and T.H. Xu, “A review of the development and characteristics of planar phase-Doppler anemometry,” *Meas. Sci. Technol.*, **8**, 1203−1221 (1997).
43. S.Y. Huang, *Modern Testing Techniques for Powder Engineering,* Huazhong University of Science & Technology Press, Wuhan (2001).
44. R.J. Adrian, “Twenty years of particle image velocimetry,” *Exp. Fluids*, **39**, 159–169 (2005).
45. B. Wieneke, “Stereo-PIV using self-calibration on particle images,” *Exp. Fluids.*, **39**, 267–280 (2005).
46. M. Zhang, Z.M. Zhang, and Y. Chen, “Experimental study on characteristics of jet field flow at nozzle outlet of sprayer, *J. Nanjing Univ. Aero. Astro*, **51**, 493–502 (2019).
47. P.K. Kirar, S.K. Soni, P.S. Kolhe, and K.C. Sahu, “An experimental investigation of droplet morphology in swirl flow,” *J. Fluid Mech.*, **938**, A6 (2022).
48. G.S.E. Antipas, “Review of gas atomisation and spray forming phenomenology,” *Powder Metall.*, **56**, 317–330 (2013).
49. J. Ting, J. Connor, and S. Ridder, “High-speed cinematography of gas-metal atomization,” *Mater. Sci. Eng. A: Struct*., **390**, 452−460 (2005).
50. G.S.E. Antipas, “Modelling of the break up mechanism in gas atomization of liquid metals. Part I: The surface wave formation model,” *Comp. Mater. Sci.*, **35**, 416–422 (2006).
51. S. Markus, U. Fritsching, and K. Bauckhage, “Jet break up of liquid metal in twin fluid atomization,” *Mater. Sci. Eng. A: Struct.*, **326**, 122–133 (2002).
52. M. Xiang, H.C. Zhou, X.Y. Zhao, and B. Liu, “Transient dynamic analysis for the ventilated supercavity under the action of tail jetting flow,” *Acta Mech. Sin.*, **38**, 321365 (2022).

53. D.I. Meiron, G.R. Baker, and S.A. Orszag, “Analytic structure of vortex sheet dynamics. Part 1. Kelvin–Helmholtz instability,” *J. Fluid Mech.*, **114**, 283−298 (1982).
54. B. Yu, L.Y. Li, H. Xu, B. Zhang, and H. Liu, “Effects of Reynolds number and Schmidt number on variable density mixing in shock bubble interaction,” *Acta Mech. Sin.*, **38**, 121256 (2022).
55. C.J. Gurney, *The Stability and Control of Curved Liquid Jet Break-up,* PhD, University of Birmingham (2010).
56. S.P. Mates and G.S. Settles, “A study of liquid metal atomization using close-coupled nozzles. Part 1: Gas dynamic behavior,” *Atomization Spray*, **15**, 19−40 (2005).
57. E.A. Ibrahim and E.T. Akpan, “Three dimensional instability of viscous liquid sheets,” *Atomization Spray*,. **6**, 649–665 (1996).
58. M. Zhang, Z.M. Zhang, and Q.S. Liu, “Research on the primary liquid atomization mechanism of a close-coupled vortical loop slit atomizer,” *Acta Mech. Sin.* **39**, 322476 (2023).
59. J. Ting and I.E. Anderson, “A computational fluid dynamics (CFD) investigation of the wake closure phenomenon,” *Mater. Sci. Eng. A: Struct.*, **379**, 264–276 (2004).
60. M. Pilch and C.A. Erdman, “Use of breakup time data and velocity history data to predict the maximum size of stable fragments for acceleration-induced breakup of a liquid-drop,” *Int. J. Multiphase Flow*, **13**, 741–757 (1987).
61. H. Zhao, H.F. Liu, W.F. Li, and J.L. Xu, “Morphological classification of low viscosity drop bag breakup in a continuous air jet stream,” *Phys. Fluids*, **22**, 114103 (2010).
62. J. Mi, R.S. Figliola, and I.E. Anderson, “A numerical simulation of gas flow field effects on high pressure gas atomization due to operating pressure variation,” *Mater. Sci. Eng. A: Struct.*, **208**, 20–29 (1996).
63. H. Liu and R. Dax, “Effect of atomizer geometry on gas flow field in gas atomization,” *Met. Powder Rep.*, **53**, 40 (1998).
64. C. Yu and I.E. Anderson, “Application of computational fluid dynamics to analyze the gas flow field of single-discrete jets,” in: J.J. Oakes and J.H. Reinshagen (Eds.), *Advances in Powder Metallurgy & Particulate Materials'98*, Proceedings of the 1998 International Conference on Powder Metallurgy & Particulate Materials, Vol. 2, Metal Powder Industry Federation, Princeton (1998).
65. P.I. Espina and U. Piomelli, “Study of the gas jet in a close-coupled gas-metal atomizer,” in: *36th AIAA Aerospace Sciences Meeting and Exhibit* (2–15 January 1998), AIAA Paper 98–0959, Reno, NV, USA (1998). https://doi.org/10.2514/6.1998-959.
66. S.Z. Chen and Z.M. Yin, “Effect of vortical nozzle on leakage pipe extension,” *Mater. Sci. Technol.*, **6**, 69–72 (1998).
67. S.Z. Chen, “Design principles of pipelines and nozzles for powder preparation by gas atomization,” *Light. Met.*, **4**, 56–59 (1998).
68. S.Z. Chen, “The factors to influence working efficiency of atomizer,” *Light Alloy Fabrication Technol*., **26**, 43–46 (1998).
69. J.F. Sun, F.Y. Cao, C.S. Cui, J. Shen, and Q.C. Li, “Dynamic behaviors of gas velocity field during metal atomization,” *Powder Metall. Technol.*, **20**, 79–81 (2002).
70. U. Fritsching, “Droplets and particles in sprays: Tailoring particle properties within spray processes,” *China Particuology*, **3**, 125–133 (2005).
71. X. Chen, *Study on the Structure of Close-Coupled Gas Atomization Flow Field and Atomization Mechanism,* PhD, Central Southern University, Changsha, China (2007).
72. N. Zeoli and S. Gu, “Computational simulation of metal droplet break-up, cooling and solidification during gas atomization,” *Comp. Mater. Sci.*, **43**, 268–278 (2008).
73. J. Ting, M.W. Peretti, and W.B. Eisen, “The effect of wake-closure phenomenon on gas atomization performance,” *Mater. Sci. Eng. A: Struct.*, **326**, 110–121 (2002).
74. M. Jeyakumar, G.S. Gupta, and S. Kumar, “Modeling of gas flow inside and outside the nozzle used in spray deposition,” *J. Mater. Proc. Technol.*, **203**, 471–479 (2008).

75. M.M. Tong and D.J. Browne, "Direct numerical simulation of melt-gas hydrodynamic interactions during the early stage of atomisation of liquid intermetallic," *J. Mater. Proc. Technol.*, **202**, 419–427 (2008).
76. A. Allimant, M.P. Planche, Y. Bailly, L. Dembinski, and C. Coddet, "Progress in gas atomization of liquid metals by means of a De Laval nozzle," *Powder Technol.*, **190**, 79–83 (2009).
77. X.M. Zhao, J. Xu, X.X. Zhu, and S.M. Zhang, "Effect of protrusion length of melt delivery tube on gas flow field for supersonic gas atomization," *T. Nonferr. Metal. Soc.*, **19**, 967–973 (2009).
78. H.W. Ouyang, Q. Wang, and Z.M. Liu, "Numerical study on abrupt change of flow field in close-coupled gas atomization," *Mater. Sci. Eng. Powder Metall.*, **15**, 96–101 (2010).
79. O. Aydin and R. Ünal, "Experimental and numerical modeling of the gas atomization nozzle for gas flow behavior," *Comput. Fluids.*, **42**, 37–43 (2011).
80. N. Zeoli, H. Tabbara, and S. Gu, "CFD modeling of primary breakup during metal powder atomization," *Chem. Eng. Sci.*, **66**, 6498–6504 (2011).
81. F.P. Liu, "Analysis on design parameters of the vortical loop slot atomizer," *Powder Metall. Technol*., **29**, 339–343 (2011).
82. W.J. Zhao, *Study on the Gas Flow Field in Spray Deposition and the Breakup Mechanism*, PhD, Harbin Institute of Technology, China (2012).
83. W.J. Zhao, F.Y. Cao, Z.L. Ning, and J.F. Sun, "Flow field simulation of double layer atomizer, *T. Nonferr. Metal. Soc.*, **19**, s485–s489 (2009).
84. W.J. Zhao, F.Y. Cao, Z.L. Ning, G.Q. Zhang, Z. Li, and J.F. Sun, "A computational fluid dynamics (CFD) investigation of the flow field and the primary atomization of the close coupled atomizer," *Comput. Chem. Eng.*, **40**, 58−66 (2012).
85. N. Zeoli, H. Tabbara, and S. Gu, "Three-dimensional simulation of primary break-up in a close-coupled atomizer," *Appl. Phys. A: Mater.*, **108**, 783–792 (2012).
86. S. Motaman, A.M. Mullis, R.F. Cochrane, I.N. McCarthy, and D.J. Borman, "Numerical and experimental modelling of back stream flow during close-coupled gas atomization," *Comput. Fluids*., **88**, 1–10 (2013).
87. J.H. Fu, *The Study of Simulation and Experimental on Effect of Four Kinds of Atomizing Gas on Gas Flow Field for Supersonic Gas Atomization,* PhD, General Research Institute for Nonferrous Metals, Beijing, China (2014).
88. S. Motaman, A.M. Mullis, R.F. Cochrane, and D.J. Borman, "Numerical and experimental investigations of the effect of melt delivery nozzle design on the open-to closed-wake transition in closed-coupled gas atomization," *Metall. Mater. Trans.*, **B46**, 1990–2004 (2015).
89. S.H. Wang, Y.C. Fang, D.G. Zhao, K.X. Zhang, and C.Y. Song, "Numerical simulation of liquid metal primary atomization in gaseous swirling flow field," *China Powder Sci. Technol.*, **22**, 7–12 (2016).
90. Y.F. Ma and Z.M. Zhang, "Simulation and analysis of gas flow field in metallic solution atomizer," *Int. J. Fluid Dynam*., **5**, 76–82 (2017).
91. D. Schwenck, N. Ellendt, J. Fischer-Buhner, P. Hofmann, and V. Uhlenwinkl, "A novel convergent-divergent annular nozzle design for close-coupled atomization," *Powder Metall.*, **60**, 198–207 (2017).
92. X.G. Li and U. Fritsching, "Process modeling pressure-swirl-gas-atomization for metal powder production," *J. Mater. Proc. Technol.*, **239**, 1–17 (2017).
93. R. Kaiser, C.G. Li, S.S. Yang, and D.G. Lee, "A numerical simulation study of the path-resolved breakup behaviors of molten metal in high-pressure gas atomization: With emphasis on the role of shock waves in the gas/molten metal interaction," *Adv. Powder Technol.*, **29**, 623–630 (2018).
94. Y.E. Kayali and R. Ünal, "Determination of metal powder particle size by numerical modeling in gas atomization," *J. Fac. Eng. Archit. Gaz*, **33**, 1135–1144 (2018).
95. K.H. Arachchilage, M. Haghshenas, S. Park, L. Zhou, Y.H. Sohn, B. McWilliams, K. Cho, and R. Kumar, "Numerical simulation of high-pressure gas atomization of two-phase flow: Effect of gas pressure on droplet size distribution," *Adv. Powder Technol.*, **30**, 2726–2732 (2019).

96. F. Hernandez, T. Riedemann, J. Tiarks, B. Kong, J.D. Regele, T. Ward, and I.E. Anderson, "Numerical simulation and validation of gas and molten metal flows in close-coupled gas atomization," in: *TMS 2019. 148th Annual Meeting & Exhibition Supplemental Proceedings*, *The Minerals, Metals & Materials Series*, Pittsburgh, USA (2019), pp. 1507–1519.
97. D. Beckers, N. Ellendt, U. Fritsching, and V. Uhlenwinkel, "Impact of process flow conditions on particle morphology in metal powder production via gas atomization," *Adv. Powder Technol.*, **31**, 300–311 (2020).
98. M. Zhang, Z.M. Zhang, Y.Q. Zhang, and Y.J. Lu, "CFD-based numerical simulation of gas flow field characteristics in close-coupled vortical loop slit gas atomization," *Atomization Spray*, **31**, 17–47 (2021).
99. M. Zhang, Z.M. Zhang, Y.Q. Zhang, Y.J. Lu, and L. Lu, "Effects of gas flow field on clogging phenomenon in close-coupled vortical loop slit gas atomization," *Trans. Nanjing Univ. Aero. Astro*., **38**, 1003–1019 (2021).
100. S. Zhang, S. Alavi, A. Kashani, Y.S. Ma, Y.X. Zhan, W.X. Dai, W.J. Li, and J. Mostaghimi, "Simulation of supersonic high-pressure gas atomizer for metal powder production," *J. Therm. Spray Technol.*, **30**, 1968–1994 (2021).
101. C. Liu, X. Li, S. Shu, Y.H. Huang, X.G. Li, and Q. Zhu, "Numerical investigation on flow process of liquid metals in melt delivery nozzle during gas atomization process for fine metal powder production," *Trans. Nonferrous Met. Soc. China*, **31**, 3192–3204 (2021).
102. S. Luo, H.Z. Wang, Z.Y. Gao, Y. Wu, and H.W. Wang, "Interaction between high-velocity gas and liquid in gas atomization revealed by a new coupled simulation model," *Mater. Design.* **212**,110264 (2021).
103. X.X. Gao, J.Y. Chen, Y.N. Qiu, Y. Ding, and J.L. Xie, "Effect of phase change on jet atomization: a direct numerical simulation study," *J. Fluid Mech.*, **935**, A16 (2022).